EDGEWOOD

CHEMICAL BIOLOGICAL CENTER

U.S. ARMY SOLDIER AND BIOLOGICAL CHEMICAL COMMAND

ECBC-TR-265

QUANTUM CHEMICAL STUDY OF THE PHOSPHITE-PHOSPHONATE TAUTOMERIZATION:

APPLICATION TO BIS(2-ETHYLHEXYL) PHOSPHONATE (BIS) AND OTHER SIMULANTS FOR CHEMICAL WARFARE AGENTS

William E. White

RESEARCH AND TECHNOLOGY DIRECTORATE

November 2002

Aberdeen Proving Ground, MD 21010-5424

Disclaimer

The findings in this report are not to be construed as an official Department of the Army position unless so designated by other authorizing documents.

REPORT DOCUMENTATION PAGE

Form Approved
OMB No. 0704-0188

1. AGENCY USE ONLY *(Leave Blank)*	2. REPORT DATE	3. REPORT TYPE AND DATES COVERED
	2002 November	Final; 01 Dec - 02 Apr

4. TITLE AND SUBTITLE
Quantum Chemical Study of the Phosphite - Phosphonate Tautomerization: Application to *bis*(2-Ethylhexyl) Phosphonate (BIS) and Other Simulants for Chemical Warfare Agents

5. FUNDING NUMBERS
PR-206023

6. AUTHOR(S)
White, William E.

7. PERFORMING ORGANIZATION NAME(S) AND ADDRESS(ES)
DIR, ECBC, ATTN: AMSSB-RRT-PC, APG, MD 21010-5424

8. PERFORMING ORGANIZATION REPORT NUMBER
ECBC-TR-265

9. SPONSORING/MONITORING AGENCY NAME(S) AND ADDRESS(ES)

10. SPONSORING/MONITORING AGENCY REPORT NUMBER

11. SUPPLEMENTARY NOTES

12a. DISTRIBUTION/AVAILABILITY STATEMENT
Approved for public release; distribution is unlimited.

12b. DISTRIBUTION CODE

13. ABSTRACT *(Maximum 200 words)*

Quantum chemical methods (ab initio, semiempirical, and Hartree-Fock) were used to calculate the energy of several phosphite - phosphonate tautomers, and thereby determine the position of equilibrium in the gas phase. Unless the phosphorus moiety contains significant electron withdrawing groups, the equilibrium lies far toward the phosphonate. None of the methods consistently produced thermodynamic values that agreed within 5 kcal/mole. In the most stable conformation of trimethyl phosphite, two of the methoxy ligands were oriented upward (with respect to the lone pair) in a pseudocistoid or *gauch* arrangement and the other pointed downward in a transoid orientation. Dimethylmethyl phosphonate (DMMP) had a similar structure. The methyl group assumed the *trans* position, and the two methoxy were in the *gauch*. The two long alkyl chains in BIS were oriented in a V fashion with the ends on the molecule about 14 angstroms apart. The vibrational spectra for trimethyl phosphite, DMMP, and *bis*(2-ethylhexyl) phosphonate were calculated at the HF/6-311G** level and compared to experimentally measured frequencies. Graphic representations of the calculated vibrations and correlation with traditional group frequencies were used to make the individual assignments.

14. SUBJECT TERMS

Chemical agent	Simulant	DMMP
Vibrational spectra	Tautomers	
bis(2-ethylhexyl) phosphonate	Quantum chemistry	

15. NUMBER OF PAGES
55

16. PRICE CODE

17. SECURITY CLASSIFICATION OF REPORT	18. SECURITY CLASSIFICATION OF THIS PAGE	19. SECURITY CLASSIFICATION OF ABSTRACT	20. LIMITATION OF ABSTRACT
UNCLASSIFIED	UNCLASSIFIED	UNCLASSIFIED	SAR

Blank

PREFACE

The work described in this report was authorized under Project No. 206023, Non-Medical CB Defense. This work started in December 2001 and was completed in April 2002.

The use of either trade or manufacturers' names in this report does not constitute an official endorsement of any commercial products. This report may not be cited for purposes of advertisement.

This report has been approved for public release. Registered users should request additional copies from the Defense Technical Information Center; unregistered users should direct such requests to the National Technical Information Center.

Acknowledgments

The help and assistance of the ECBC library staff are greatly appreciated. Corky Smith and Patsy D'Eramo performed numerous literature searches to locate government reports and open literature articles that are described in this manuscript. Carolyn Sullivan obtained several books and journal articles quickly via interlibrary loan. Ed Gier responded to frequent requests and provided information quickly in a useful format.

I also wish to acknowledge the assistance of Patricia Reeves and Sandra Johnson in the Technical Releases Office. Both provided considerable editorial advice and guidance on formatting the manuscript and citation of references.

Blank

Contents

Tables

Quantum Chemical Study of the Phosphite – Phosphonate Tautomerization:

Application to *bis*(2-Ethylhexyl) Phosphonate (BIS) and Other Simulants for Chemical Warfare Agents

1. INTRODUCTION

For many years, *bis*(2-ethylhexyl) phosphonate (BIS) has been used as a simulant for chemical warfare (CW) agents having low volatility. In earlier technical reports, the compound may be named *bis*(2-ethylhexyl) hydrogen phosphonate or *bis*(2-ethylhexyl)

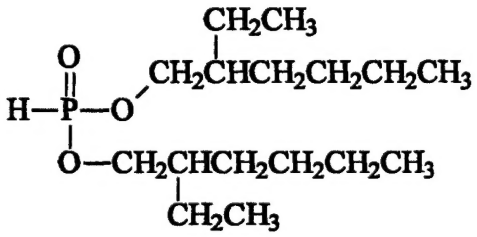

Bis(2-Ethylhexyl) phosphonate

hydrogen phosphite. It was originally selected for use as an aerosol to study the dissemination of low volatile chemical agents such as VX from exploding and other munitions.[1] BIS was a very useful simulant in the 1950's and '60's because of ease of analysis. The droplets could be collected in small pans positioned around the test sight and analyzed by reacting with trinitrobenzene. The resulting adduct/complex was quantitated photometrically by measuring its absorbance with a Klett-Sommerson colorimeter equipped with a 660 nm filter.

The original report on the analytical methodology attributed the color to the reaction of the enol form of BIS with trinitrobenzene in a basic solution.[2]

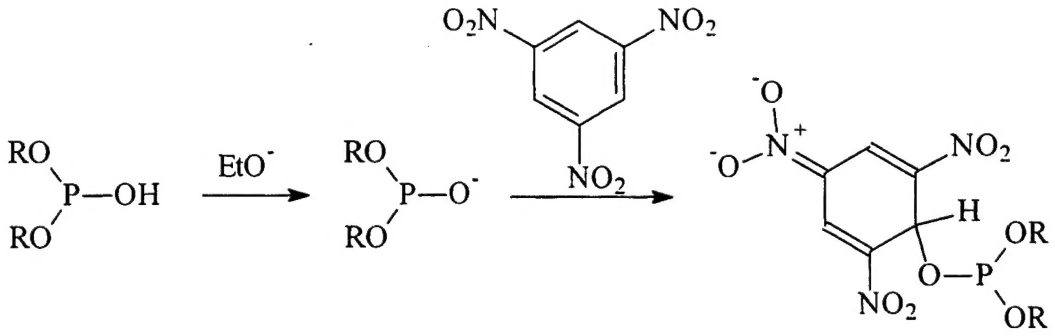

Similar colors could be obtained with other phosphonates such as dimethyl phosphonate and di n-butyl phosphonate.

The position of the equilibrium between the phosphite and phosphonate tautomers is important because BIS will continue to be used as a simulant in the development of new sensors utilizing infrared spectroscopy as the basis of detection. The dipole moments of the tautomers differs considerably so the interactions with surfaces – particularly those with acidic or basic functionalities – may be different.

Usually, the equilibrium lies far toward the phosphonate for compounds having a P—H or P—OH group.[3] Phosphonic acid may be the best example. The equilibrium lies so far

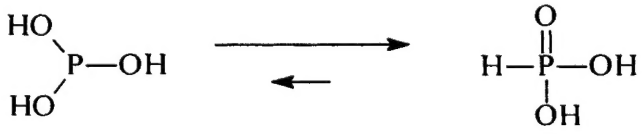

to the right that only two hydrogens are titratable even though the first and second dissociation constants are greater than for tribasic phosphoric acid. The measured dissociation constants for phosphorus acid are listed in Table 1. When the enol concentration is less than 1ppm, traditional methods of analysis become very difficult.[4] For phosphonic acid, the hydrogen/deuterium exchange of the two titratable hydrogens is almost instantaneous. In contrast, the half life for exchange of the third hydrogen is about 200 minutes at 23° C under neutral conditions based on Raman scattering for the P—H and P—D vibrations at 2457 and 1793 cm^{-1} respectively.[5] The rate is faster in acid – presumably involving the protonation of the phosphonyl oxygen and rapid dissociation of the P—H bond. The proton exchange is also subject to general base catalysis – presumably caused by removal of the phosphorus proton and acidification of all oxygens.

Table 1. Dissociation Constants of Phosphorus Acids[6]

	Phosphinic Acid	Phosphonic Acid	Phosphoric Acid
pKa_1	1.1	1.3	2.1
pKa_2	--	6.7	7.2
pKa_3	--	--	12.7

In contrast to the phosphorus acids in Table 1, The dissociation constant for diethyl phosphonate[7] is 2.5×10^{-15} which places it in the range of the dissociation of ethanol. Lewis and Spears were not able to determine whether the dissociation resulted from the weak dissociation of the phosphonate in high concentration or from the moderately strong dissociation for the phosphite in low concentration.

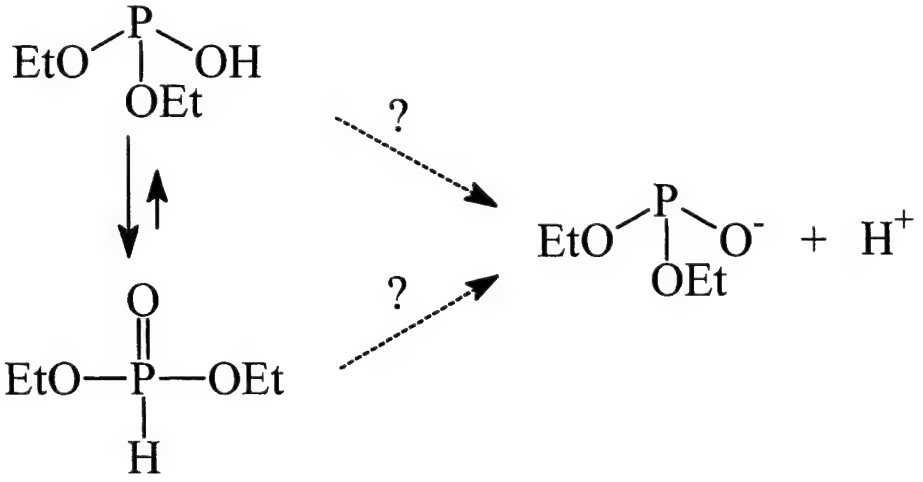

The tautomeric equilibrium constant for phosphorus acid and related compounds have not been measured; however, they have been calculated from available thermodynamic data. Table 2 lists some that were generated by Guthrie.[8]

Table 2. Tautomeric Equilibria[8]

Reaction			log K
$P(OEt)_2OH$	→	$HPO(OEt)_2$	7.2
$P(OEt)(OH)_2$	→	$HPO(OEt)(OH)$	8.7
$P(OH)_3$	→	$HPO(OH)_2$	10.3
$P(OEt)(OH)(O-)$	→	$HP(O)_2(OEt)-$	14.5

In contrast to phosphorus esters, the trialkyl and triaryl analogs can exist in both tautomers. Both trimethyl phosphite and dimethyl methylphosphonate are readily available commercially from Aldrich as well as other chemical supply houses.

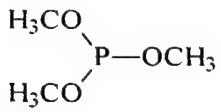

Trimethyl phosphite

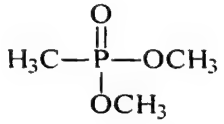

Dimethyl methylphosphonate

The heats of formation have been measured[9,10] for both compounds so it is possible to calculate their relative concentration at equilibrium. Similar thermodynamic properties have not been measured for *bis*(2-ethylhexyl) phosphonate. It is possible that the large alkyl groups on 2-ethylhexyl phosphonate could alter the equilibrium by exerting some type of electronic or, more likely, a steric effect. If the trigonal phosphorus could become more planer, the large alkyl groups could be more dispersed than in the tetragonal or pyramidal structures.

To test this hypothesis, both tautomers of *bis*(2-ethylhexyl) phosphonate were examined quantum chemically at the restricted Hartree-Fock level of theory using both semiempirical and ab initio methods. To gain additional perspective, the phosphonic acid and trimethyl phosphite systems were studied with the same methods.

2. METHODOLOGY

2.1 Calculations

Semiempirical calculations using the AM1and PM3, Hamiltonians and associated parameters were performed on an SGI O2 workstation using AMPAC 6.55. [11] Optimization was performed with the TRUST routine. Frequency calculations were performed on all optimized structures to confirm that the stationary points were minima and thereby corresponded to stable structures (no negative frequencies in the Hessian matrix) and not transition states (one negative frequency corresponding to the reaction path) or other higher order conformations. In general, the default parameters within AMPAC were employed. The input geometries were generated by the AMPAC Graphical User Interface (AGUI). AGUI was also used to view the optimized structures and determine the bond lengths, angles and dihedrals.

Ab initio calculations were performed with Gaussian 98 version A.9[12] on the multinode SGI Origin 2000 at the ARL High Performance Computing Center. Structures were optimized with the Berny[13] routine using 4 parallel processors. The input matrix was created with Gaussview 2.0. Quantum calculations were run at the restricted Hartree Fock level of theory with the following basis sets: 3-21G*, 6-31G*, and 6-311G** and 2nd and 4th order Møller-Plesset perturbation (MP2 and MP4) using the 6-31G* basis set. Density functional theory calculations were also run with the 6-31G* basis set using the

3BLYP hybrid functional. Compound calculations using the CBS-Q model were run on trimethyl phosphite and DMMP. Diffuse functions were not employed in any calculations because none of the structures examined were ionized. Frequency calculations were performed on all optimized structures to confirm that the stationary points were minima. Calculations were performed on isolated molecules (gas phase) without any solvation models. Output was visualized with Gaussview in a manner similar to that used with AGUI for the semiempirical results.

2.2 Partial charges

2.2.1 Analysis of electron population within the molecule

The charge on an atom is the sum of the protons minus the electrons. The protons are localized within the nucleus and essentially remain constant. In contrast, the electron cloud surrounding an atom may change considerably as a result of formation of chemical bonds and other electrostatic interactions. Therefore, the major problem associated with the determination of the partial or effective charge on an atom in a molecule is the localization of the electron distribution within a molecule and its assignment to specific atoms. Because atomic charge is not a direct product of the solution to the wave equation, some method must be devised to separate the electron density into local units corresponding to the atoms comprising the molecule.[14] Because the accuracy of the results cannot be evaluated empirically, the choice of approach is arbitrary. The most commonly used method for determining atomic charges within a molecule was developed by Mulliken in the early 1950's.[15] Even though it enjoys great popularity, it is the subject of intense criticism as a consequence of it deficiencies. Unfortunately, no current method is entirely satisfactory. The results from three different methods are included in this paper. They are briefly described below.

2.2.2 Basis Function Derived Methods

The electron density function is the probability that an electron is occupying a designated small volume. Its three dimensional integral over all space equals the number of electrons in the molecule.[16] This integral can be divided into a matrix composed of the products of two components commonly designated P_{xy} and S_{xy}. P is the density matrix and S is the overlap matrix between atoms x and y. The Mulliken method uses a PS matrix to assign the partial charge on each atom.[15,17-19] If x and y are the same, then the overlap is one and the product is P. These diagonal elements of the matrix describe the electrons that reside almost exclusively on individual atoms such as core and non-bonding electrons. The off diagonal elements ($x \neq y$) describe the degree to which the electrons are shared and collectively constitute the overlap population. In the Mulliken method, the electron densities in the off diagonal elements are divided evenly between the two atoms. This may be appropriate when the electronegativity on both atoms is similar such as in a C—C bond; but seems inappropriate for a C—F bond. The electron

density is the sum of the P_{xx} element and of all the $P_{xy}S_{xy}$ elements. The Mulliken charge is the sum of the nuclear and electronic charges.

As can be inferred, the results depend upon the overlap of electrons, which depend upon the basis set. Therefore the Mulliken charges are very basis set dependent, and it is inappropriate to compare Mulliken charges generated with one basis set with those computed with another. Sometimes, the electron density can be a negative number. This may not pose a mathematical problem; however, the physical meaning of negative electron density is difficult to comprehend and tends to discredit the method. A third problem is the difficulty obtaining reasonable results on compounds having substantial ionic character. The Lőwdin method eliminates some of these problems but has never been as popular as Mulliken.

2.2.3 Fitting Atomic Charge to Electrostatic Potential

The electrostatic surface of a molecule is generated by determining the electrostatic potential at numerous sites.[20] Then trial atomic charges on each atom at its specific locus within the molecule are fitted to generate the potential surface.[21] It the past, the surface fitting procedure could be quite computationally expensive. In the CHELP program, the computation time was shortened considerably by using a Lagrangian multiplier to effect the least squares fit.[22] The program generated the surface defining matrix with 14 points surrounding each atom. Points within the van der Waals radii were removed. Because the results from the original CHELP program depended on the orientation of the points, different conformations had considerably different partial charges. This problem was eliminated in the CHELPG program by generating the matrix from a series of points evenly distributed through the molecule.[23] The number of points is usually about 3000 in contrast to 300 for the original CHELP calculation. In general, the partial charges from CHELPG and other electrostatic methods are less sensitive to basis sets.

2.2.4 Natural Orbitals

Another approach involves the use of natural orbitals.[24] NBO analysis was developed to study hybridization and covalent bonding in large wave functions. It was conceived as the "Chemist's Basis Set" that would resemble the chemist view of bonds and electron lone pairs. In this method, the shapes of atomic orbitals in the molecule are described or defined by the one electron density matrix.[25] Then, the molecular bonds and atomic charges can be obtained. After the density matrix has been transformed, the program searches for natural Lewis structures. The high occupancy orbitals (~2 electrons) are designated unhybridized core orbitals. The program then looks for lone pairs whose occupancy exceeds 1.90. The two center bonds having an occupancy greater than the threshold are identified and subsequently separated into their atomic hybrids. Finally, the low-density Rydberg orbitals are examined. The atomic charge on each atom is the sum

of all 4 components. Because the electron density in the core orbitals is close to two and the Rydberg populations are normally small, most of the variation in atomic charge results from differences in the valance electrons.

2.2.5 Atoms in Molecules

In some respects the charges generated by the Atoms in Molecules (AIM) program developed by R.F.W. Bader are the best.[26] This method is very good at representing the polarization of H—C bonds. The results can be favorably compared with empirical data derived from x-ray crystallography. The method also permits calculation of additional properties of atoms such as kinetic and potential energies as well as NMR shifts.

In the AIM method, various atomic regions are identified from the shape of the charge distribution surface.[14] Frequently, electron density is maximal at the atomic centers. Critical points are located between atoms that have minimal electron density along the bond but where the electron density is maximal in other directions, i.e., a saddle point. The paths of decreasing density are evaluated to generate a zero flux surface. These zero flux surfaces are used to separate the molecule into atomic regions. Finally integration of the electron density within each region affords the atomic charge for that region and hence for the atom occupying it.

Unfortunately, the electron density surface caused by the P—F bonds is frequently too steep or contains other topological features that preclude successful completion of the AIM program. Frequently, calculations on these compounds abort or terminate prematurely. Because much interest involves organophosphorus compounds containing P—F bonds, the decision was made to used the other methods for determination of partial charge so results could be compared more easily.

3. RESULTS

Before beginning extensive computational studies, it is useful to conduct preliminary calculations on smaller, but related compounds, whose geometries have been determined experimentally. The plan for this effort is to perform a series of calculations at various levels of theory on some test molecules to determine the optimal level of theory and then examine *bis*(2-ethylhexyl) phosphonate at that level.

3.1 *Small Phosphorus Compounds*

Phosphorus trichloride is an example of a trivalent phosphorus compound having a pyramidal geometry. Phosphorus oxychloride is a pentavalent (or tetravalent depending on individual perspective) compound having a distorted tetrahedral geometry. In Table 3, the geometric parameters determined experimentally are compared with those calculated at various levels of theory.

Table 3. Geometries of Phosphorus Chlorides at Different Levels of Theory

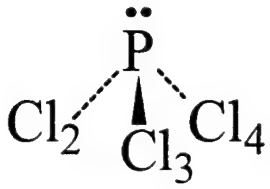

Geometric Parameter	Experimental (Reference[27])	AM1	PM3	HF/ 3-31G*	HF/ 6-31G*	MP2/ 6-31G*
P—Cl	2.043	1.919	2.064	2.039	2.049	2.055
Cl-P-Cl	100	105.43	99.69	100.45	100.75	101.06
Cl-P-Cl-Cl		-111.3	101.68	-102.8	-103.3	-103.7

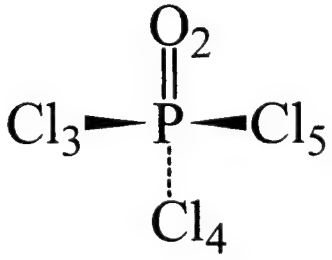

Geometric Parameter	Experimental (Reference[28])	AM1	PM3	HF/ 3-21G*	HF/ 6-31G*	MP2/ 6-31G*
P—O	1.449	1.465	1.415	1.447	1.440	1.477
P—Cl	2.002	1.944	2.032	1.984	1.997	2.010
Cl-P-Cl	104	103.74	101.17	103.49	103.95	103.52
O-P-Cl		114.72	116.86	114.94	114.54	114.91
Cl-P-Cl-Cl		108.2	103.9	107.7	108.5	107.7

All computational methods indicate that phosphorus trichloride (PCl_3) has C_{3v} symmetry with the electron lone pair located at the apex of the trigonal pyramid. All methods give good P—Cl bond lengths. The semiempirical method AM1 generates the shortest at 1.919 Å and the second order Møller-Plesset (MP2) produces the longest at 2.055Å. The experimental value of 2.043 Å is only 6 thousands of an Angstrom smaller than

HF/6-31G*. The AM1 bond angles are larger (105°) than experimental (100°). The three ab initio methods agree exactly. Both experimental and calculated bond angles indicate that the lone pair occupies a larger area than the chlorides and thereby compresses them slightly on one side of the molecule. This feature is indicated by the 100° bond angle and the Cl-P-Cl-Cl torsional angles of 100° and 103° respectively. The analogous values are 109.5° and 120° for a tetrahedron.

Phosphorus oxychloride also has C_{3v} symmetry with the phosphorus lone pair involved in the formation of the P=O bond. The experimental bond lengths for the P=O bond are slightly longer than experimental with AM1 and MP2 but almost exact with the 2 basis sets at the Hartree-Fock level. All methods generate the correct Cl-P-Cl bond angle. The larger bond angle (100°) indicates that the oxygen in $POCl_3$ occupies less space than the lone pair in PCl_3. This phenomenon is also seen in the larger Cl-P-Cl-Cl torsional angle of 108°.

All levels of theory examined generate acceptable geometries for PCl_3 and $POCl_3$. The accuracy of the energy calculations was not determined here; however, they usually improve with increasing size of the basis set. In general, MP2 calculations provide more accurate energies than Hartree-Fock calculations. With a reasonable basis set, the energies from ab initio methods are usually superior to semiempirical methods.

3.2 *Phosphonic Acid*

The calculated energies of the tautomers of phosphonic acid are delineated in Table 4.

Table 4. Energies of $P(OH)_3$ and $HP(O)(OH)_2$

Method	Phosphite	Phosphonate	Difference (kcal/mole)	Gas Phase Population Ratio Phosphite/Phosphonate
AM1 (kcal/mole)	-218.70	-204.87	(13.83)	$7.2 \times 10^{-11}/1$
PM3 (kcal/mole)	-223.50	-209.09	(14.41)	$2.7 \times 10^{-11}/1$
HF/3-21G* (Hartrees)	-564.2682	-564.2827	9.09	$1 / 2.15 \times 10^{-7}$
HF/6-31G* (Hartrees)	-567.1002	-567.1174	10.79	$1 / 1.2 \times 10^{-8}$
HF/6-311G**	-567.2014	-567.2143	8.09	$1 / 1.2 \times 10^{-6}$
MP2/6-31G*	-567.7473	-567.7651	11.17	$1 / 6.0 \times 10^{-9}$

The values from the semiempirical calculations (i.e., AM1 and PM3) indicating the heats of formation are expressed in kcal/mole. Results from the ab initio calculations represent the total energy in the system and are expressed in Hartrees. One Hartree equals 627.5 kcal. All values in the "Difference" column are expressed in kcal/mole. The gas phase population at 25° C was calculated from the Boltzman distribution as described in the Methods section.

The most apparent feature in Table 4 is the qualitative difference between the ab initio and semiempirical results. It is usually conceded that semiempirical methods generate accurate geometries for traditional compounds; however, the truncated Hamiltonian is too small for accurate absolute energies. Nevertheless, semiempirical methods usually provide accurate relative energies between different molecules because many of the intrinsic errors cancel. Such was not the case here. It was very surprising that the semiempirical heats of formation (both AM1 and PM3) for the phosphite tautomer was less than the phosphonate. The ab initio results were qualitatively correct and the ratio of phosphonate increased with the basis set and level of theory.

Rather than the total energy, the Gibbs free energy may be a better parameter for comparing energy differences between tautomers because entropy contributions are removed. They can be calculated directly by the Gaussian program.[29] In Table 5, the Gibbs free energies are included for the ab initio methods.

Table 5. Gibbs Free Energies of $P(OH)_3$ and $HP(O)(OH)_2$

Method	Phosphite Tautomer (Hartrees)	Phosphonate Tautomer (Hartrees)	Difference (kcal/mole)	Gas Phase Population Ratio Phosphite/Phosphonate
HF/3-21G*	-564.250852	-564.264578	8.613	4.8×10^{-7} / 1
HF/6-31G*	-567.081807	-567.097756	10.00	4.6×10^{-8} / 1
HF/6-311G**	-567.182374	-567.195240	8.07	1.2×10^{-6} / 1
MP2/6-31G*	-567.732370	-567.749031	10.45	2.1×10^{-8} / 1

The geometric and electronic parameters of the phosphite tautomer calculated at various levels of theory are listed in Table 6.

Table 6. Calculated Geometry of $P(OH)_3$

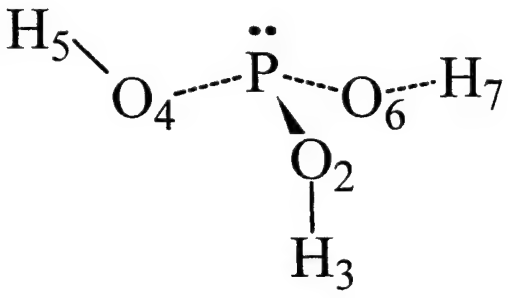

Geometric Parameter	AM1	HF/ 3-21G*	HF/6-31G*	HF/6-311G**	MP2/6-31G*
P—O2	1.624	1.634	1.608	1.600	1.650
P—O4	1.624	1.611	1.638	1.629	1.678
P—O6	1.624	1.611	1.629	1.621	1.648
P-O2-H3	110.34	119.02	113.47	115.09	112.74
P-O4-H5	121.09	120.85	112.09	113.19	111.32
P-O6-H7	110.33	118.91	113.46	114.83	111.59
O2-P-O4	95.17	99.75	103.12	102.83	101.23
O2-P-O6	95.15	95.01	96.69	96.76	103.53
O4-P-O6	95.19	102.69	96.14	96.68	92.92
O2-P-O4-O6	-95	97	-98	-98	-104
O6-O4-O2-H3	-140	-147	-78	-79	-87
O6-O2-O4-H5	50	-94	-145	-145	-154
O2-O4-O6-H7	41	-66	-175	-170	124

Bond Orders

Bond	AM1	HF/3-21G*	HF/6-31G*	HF/6-311G**	MP2/6-31G*
P—O2	.884	.621	.705	.745	.689
P—O4	.885	.722	.664	.709	.647
P—O6	.885	.722	.671	.716	.689

Table 6 (Continued). Calculated Geometry of $P(OH)_3$

Partial Charges

Atom	AM1 Coulson	HF/6-31G* CHELP	HF/6-31G* Natural	HF/6-31G* Mulliken
P	1.002	.253	1.733	1.080
O2	-.575	-.497	-1.080	-.800
O4	-.575	-.533	-1.093	-.845
O6	-.575	-.514	-1.088	-.837

The orientation of the hydrogens in the phosphite structure depended on the basis set. With AM1 and HF/3-21G*, H5 and H7 were up (i.e., toward the phosphorus) with respect to the plane formed by the three oxygens. With HF/6-31G*, H5 was essentially in the plane as indicated by the O2-O4-O6-H7 dihedral angle of 175°. H3 was oriented down and H7 was up. The P—OH bond lengths were different for each of the three orientations of the hydrogen.

The geometry etc. for phosphonic acid is indicated in Table 7. The phosphorus is almost tetrahedral. The oxygen ligands are slightly expanded leading and crowding into the hydrogen area as indicated by the O3-P-O4-O6 dihedral angle of 126°. An angle of 120° is tetrahedral; whereas 180° is planer. The two hydroxyls are oriented away from the phosphonyl hydrogen and toward the phosphonyl oxygen. This can be seen in the O3-P-O4-H5 and O3-P-O6-H7 dihedrals of 20 and –4 degrees respectively. The P=O bond is considerably shorter than the two P—O bonds. The phosphonate tautomer is also more polar than the phosphite. There is considerably less electron density on the phosphorus and more on the oxygens.

Table 7. Geometry and Electronic Parameters for Phosphonic Acid

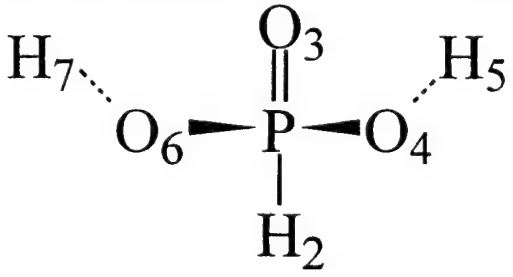

Parameter	AM1	HF/3-21G*	HF/6-31G*	HF/6-311G**	MP2/6-31G*
P —H2	1.274	1.365	1.372	1.378	1.392
P—O3	1.454	1.457	1.453	1.447	1.484
P—O4	1.595	1.580	1.586	1.575	1.614

Table 7 (Continued). Geometry and Electronic Parameters for Phosphonic Acid

P—O6	1.595	1.580	1.589	1.583	1.626
P-O4-H5	116.37	120.29	113.10	115.60	112.17
P-O6-H7	116.38	120.35	112.31	113.62	109.48
O3-P-H2	122.75	119.43	118.16	117.66	117.44
O3-P-O4	109.79	114.06	114.99	116.07	118.75
O3-P-O6	109.79	114.09	113.73	113.31	113.61
O3-P-O4-H5	15	19	19	31	50
O3-P-O6-H7	-15	-19	-3	-6	12
O3-P-O4-O6	117	126	-126	127	126
O3-O4-O6-H7	-63	-68	-49	40	-30
O3-O6-O4-H5	63	68	64	75	87

Bond Orders

	AM1	HF/3-21G*	HF/6-31G*	HF/6-311G**	MP2/6-31G*
P—H2	.705	.866	.890	.881	.891
P—O3	1.166	1.293	1.193	1.235	1.202
P—O4	.676	.698	.685	.724	.682
P—O6	.676	.698	.679	.710	.682

Partial Charges

Atom	AM1 Coulson	HF/6-31G* CHELP	HF/6-31G* Natural	HF/6-31G* Mulliken
P	2.619	1.255	2.428	1.376
H2	-.460	-.043	.137	-.070
O3	-.805	-.765	-1.196	-.720
O5	-.805	-.686	-1.079	-.783
O7	-1.109	-.691	-1.082	-.788

Because the phosphonic acid tautomer has a phosphorus-hydrogen bond, there is the possibility of distortion of the electron cloud around the hydrogen that could effect the calculated energy of the molecule. A larger basis set (i.e., 6-311G**) containing polarization functions on hydrogen as well as on the heavy atoms was used to evaluate any polarization effects on the light atoms. As would be expected, the calculated energy was slightly less for this triple zeta quality basis set; but the geometry was essentially the same. The bond angles on the hydroxyls (i.e., P—O—H) were about 1.5° larger than with the 6-31G* basis set. The P—H bond order decreased about 0.01 bond unit – thereby indicating a more polarized bond with less electron density between the nuclei.

At the Hartree-Fock level of theory, the interactions between electrons are essentially ignored. With currently available hardware and software, it is not possible to include all electron interactions on molecules the size of the smallest organophosphate. Perturbation theory has been used to address the problem of electron interaction by including terms that describe how the presence of one or more electrons affects or alters the environment of the others.[30] A frequently used procedure is to optimize the geometry at the Hartree-Fock level and then perform a single point calculation at the MP2 or higher level. In this study the small size of phosphonic acid and the availability of powerful computational hardware, permitted optimization of the geometry at the MP2 level on both tautomers using the 6-31G* basis set. The geometries generated at the Møller-Plesset level of theory differed slightly from those at the Hartree-Fock level even with the same basis set.

For the phosphonate tautomer, the overall geometries were the same at both levels of theory. The bond lengths were longer with MP2 than with HF and the P—O—H bond angles were smaller. Both changes in geometry indicate a greater p content in the bonds. The bond orders for the four phosphorus bonds are the same.

The geometries of the most stable conformation of the phosphite tautomers are basis set dependent. The pyramidal structure was consistent in all calculations with the three oxygens on one side of the molecule. The three oxygens are slightly less constricted with O2-P-O4-O6 dihedral angle of -104°. At the HF level, two of the hydrogens are oriented up toward the lone pair and one is oriented down and away from the phosphorus. At the MP2 level, only one hydrogen (H5) is oriented up and two (H3 and H7) are down. In the input geometry, H7 had an upward orientation but moved to a down position during optimization. This shift in orientation is indicated by the change of the O2-O4-O6-H7 dihedral from –175° to 124. As was seen at the HF level, the P—O bond orders for the two oxygens having downward hydrogens are greater (.689) than for the oxygen having an upward one (.647).

3.3 Fluorinated Phosphines

In contrast to most H-phosphonates, *bis*(trifluoromethyl) phosphinous acid exists principally as the trivalent tautomer rather than the tetra or pentavalent phosphine oxide.[31,32]

This compound with the opposite tautomeric equilibrium provides a good opportunity to check the computational system for gross systematic errors. The energies of the two tautomers determined at different levels of theory and the resulting populations are listed in Table 8.

Table 8. Population of $(CF_3)_2POH$

Method	$(CF_3)_2POH$	$P(CF_3)_2P(O)H$	Difference (kcal/mole)	Gas Phase Population Ratio Phosphite/Phosphonate
AM1	-347.32 (kcal/mole)	-326.80 (kcal/mole)	20.52	$1 / 8.90 \times 10^{-16}$
PM3	-355.39 (kcal/mole)	-348.70 (kcal/mole)	6.69	$1 / 1.23 \times 10^{-5}$
HF/3-21G*	-1082.8832 Har	-1082.8715 Har	7.34	$1 / 4.13 \times 10^{-6}$
HF/6-31G*	-1088.5352 Har	-1088.5246 Har	6.65	$1 / 1.32 \times 10^{-5}$

All 4 methods indicate that the phosphite tautomer is more stable than the phosphonate. PM3, HF/3-21G*, and HF/6-31G* have energy differences about 7 kcal/mol. In contrast, the AM1 result is considerably different from the other results with a difference greater than 20 kcal/mole. The reason for the AM1 discrepancy was not apparent in the geometry or electronic structures of the two tautomers.

3.4 *Trimethyl Phosphite and Dimethyl Methylphosphonate*

In contrast to phosphonic acid, the trialkyl esters can exist in each tautomer. Trimethyl phosphite is available from many chemical supply companies. It and analogous esters are easily prepared by reaction of alcohols with phosphorus trichloride. Dimethyl methylphosphonate is conveniently prepared from trimethyl phosphite and a methyl halide via the Arbusov reaction. An internal Arbusov reaction of trimethyl phosphite leads to the same product. The energetics and reaction pathway for the conversion of trimethyl phosphite into dimethyl methylphosphonate is beyond the scope of this paper. It appears that the reaction barrier is sufficiently high to preclude establishment of an equilibrium at ambient temperatures within a reasonable time. The conversion does occur at room temperature on silicas such as Cab-O-Sil© as a result of acidic catalysis of the Si-OH group.[33]

3.4.1 Trimethyl Phosphite Conformations

Trimethyl phosphite can conceivably exist in a number of conformations. In this report, the trimethyl phosphite molecule is oriented with the three oxygen atoms forming a plane below the phosphorus and the phosphorus lone pair above. Four of the most obvious conformers are indicated below in Table 9. In structure A, all methyl groups are oriented

upward. In B, one methyl is down and two are up. C and D have two and three methyl groups down respectively. Calculations were performed at the HF/6-31G* to determine the relative energies of the four conformations.

Table 9. Structures and Energies of Trimethylphosphite Conformations

A B C D

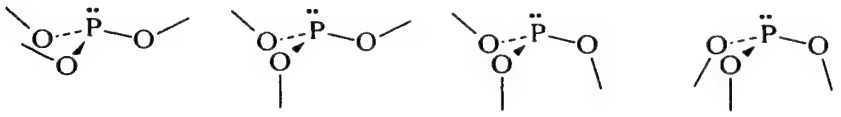

Structure #	Total Energy (Hartrees)	Gibbs Free Energy (Hartrees)	Relative Energy (kcal/mole)	Fraction
A	-684.1688	-684.060791	6.37	2.1×10^{-5}
B	-684.17442	-684.070950	0.00	.95
C	-684.1722	-684.068213	1.71	.055
D	-684.1652	-684.066101	3.04	.0059

Conformation B with two of the methyl groups oriented essentially away from the phosphorus is a pseudo *trans* position. The third methyl is oriented down in a pseudo *cis* arrangement. This conformation allows maximal separation of the methyl groups. About 5% of the population is in the C conformation with two methyl groups down and one up. Conformation A is the least stable with an equilibrium population of 10^{-5}; however, the energy level of 6 kcal/mole greater than the most stable conformer is relatively small so this conformation would not be precluded in the formation of some Lewis base complex or other intermolecular interactions.

Raman spectroscopy was consistent with the premise that in the liquid state as well as a crystaline solid at low temperatures, trimethyl phosphite exists principally as a mixture of conformers.[34] In contrast to the theoretical calculations, the data was more consistent with a larger population of conformers A and B.

3.4.2 Energies of Trimethyl Phosphite and Dimethyl Methyl Phosphonate

The relative total energies of trimethyl phosphite and dimethyl methyl phosphonate are listed in Table 10. All methods indicate that the phosphonate tautomer is the more stable.

Similar results are seen with the Gibbs free energies in Table 11. With the Gibbs free energies, the energy differences between tautomers decreases slightly but not sufficiently to alter the results.

Table 10. Total Energies and Equilibrium Population of Trimethyl Phosphite and Dimethyl Methylphosphonate

Level of Theory	Trimethyl phosphite	Dimethyl methyl phosphonate	Energy Difference (kcal/mole)	Gas Phase Population Ratio Phosphite/Phosphonate
Experimental	-177.1 (Ref 10)	-196.4 (Ref 9)	19.3	7.0×10^{-15} / 1
AM1 (kcal/mole)	-188.24	-207.42	19.18	1.56×10^{-15} / 1
PM3 (Kcal/mole)	-188.81	-190.39	1.58	.069 / 1
HF/3-21G* (Hartrees)	-680.7021	-680.7561	33.88	1.41×10^{-25} / 1
HF/6-31G* (Hartrees)	-684.1744	-684.2213	29.44	2.55×10^{-22} / 1
HF/6-311G**	-684.2883	-684.3351	29.36	2.92×10^{-22} / 1
MP2/6-311G**// HF/6-311G**	-685.4421	-685.4938	32.44	1.60×10^{-24} / 1
MP3/6-311G**// HF/6-311G**	-685.4803	-685.5261	28.76	8.08×10^{-22} / 1
MP4D/6-311G**// HF/6-311G**	-685.5077	-685.5523	27.98	3.00×10^{-21} / 1
MP4DQ/6-311G**// HF/6-311G**	-685.5895	-685.5345	28.27	1.83×10^{-21} / 1
MP4SDQ/6-311G**// HF/6-311G**	-685.5019	-685.5474	28.60	1.05×10^{-21} / 1

Table 10 (Continued). Total Energies and Equilibrium Population of Trimethyl Phosphite and Dimethyl Methylphosphonate

MP4SDTQ/6-311G**// HF/6-311G**	-685.5421	-685.5887	29.25	3.50×10^{-22} / 1
B3LYP/6-31G*	-686.77933	-686.82002	25.53	1.87×10^{-19} /1

Experimental results from thermochemical measurements indicate the phosphonate is more stable by 19 kcal/mole. This difference translates to a equilibrium population difference of 5×10^{-15}. This value is almost identical to the AM1 value; however, the values for trimethyl phosphite and dimethyl methylphosphonate differ considerably from experimental values. Because both errors are in the same direction, relative differences in AM1 calculations are frequently accurate because systematic errors tend to cancel. Unfortunately, this is not always the case. With PM3 the value for trimethyl phosphite is smaller than experimental; whereas the DMMP value is greater – thereby generating a large relative error. The HF/6-31G* value is also off by 10 kcal/ mole, which is a large value for this degree of rigor.

Single point Møeller-Plesset calculations were performed with HF/6-311G** geometries. In all cases, the energy of both phosphite and phosphonate tautomers decreases with increasing levels of theory. The lowest energies were obtained with the MP4 SDTQ level. The energy difference between the tautomers did not change significantly. The smallest difference (27.98 kcal/mole) was with the MP4 D method. The largest (32.44 kcal/mole) was with MP2. Increasing the rigor of the calculations beyond the HF level reduces the energies of the individual species; however, there is little change in the relative energy differences and the population of each tautomer.

Table 11. Gibbs Free Energies and Equilibrium Population of Trimethyl Phosphite and Dimethyl Methylphosphonate

Level of Theory	Phosphite	Phosphonate	Difference (kcal/mole)	Ratio
HF/3-21G*	-680.599554 Har	-680.652132 Har	32.99	6.36×10^{-25} /1
HF/6-31G*	-684.070950 Har	-684.117473 Har	29.19	3.90×10^{-22} /1
HF/6-311G**	-684.18666 Har	-684.23282 Har	28.97	5.65×10^{-22} /1
MP2/6-311G**// HF/6-311G**	-685.34170 Har	-685.39376 Har	32.66	1.10×10^{-24} /1

For ab initio calculations, the greatest source of error in thermodynamic calculations is caused by truncation of the basis sets. The magnitude of some errors can be reduced by conducting a series of calculations and combining the results to produce a more accurate value. The energies from G1 model were usually around 2 kcal/mole for a series of 31 test compounds.[35] Accuracy improved to about 1.5 kcal/mole in the subsequent G2 method.[36]

The complete basis set (CBS) procedures, developed by George Petersson and his associates eliminates some of the technical problems inherent in the G2 model and appears to hold greater promise.[37] The CBS-4 method is less computer intensive (about one fourth the time) than CBS-Q. A 1995 paper indicated that CBS-4 was appropriate for structures containing no more than 12 non hydrogen atoms; whereas, CBS-Q was limited to six.[38] CBS-4 begins by optimizing the structure at the HF/3-21G* level before moving to more rigorous calculations. In contrast, "The CBS-Q starts with a geometry optimization at the MP2 level of theory; the zero-point energy is computed at the HF level. It then uses a large basis set MP2 calculation as a base energy, and a CBS extrapolation to correct the energy through second order. Two additional calculations are used to approximate higher order contributions: MP4(SDQ)/6-31+(d,p) (with extra polarization functions on sulfur, phosphorus, and chlorine) to approximate the higher order correlation effects, and QCISD(T)/6-31+G† for still higher order effects. This model also has empirical corrections for spin contamination and a size-consistent higher order correction."[39] Results of the CBS-Q calculations are shown in Table 12.

Table 12. Energies for Phosphite and Phosphonate Tautomers Calculated by CBS-Q

Category	Phosphite (Hartrees)	Phosphonate (Hartrees)	Difference (kcal/mole)	Gas Phase Population Ratio Phosphite/Phosphonate
CBS-Q (0°K)	-685.84501	-685.90280	36.26	2.52×10^{-27} / 1
Energy	-685.83483	-685.89293	36.46	1.82×10^{-27} / 1
Enthalpy	-685.83389	-685.89199	36.46	1.82×10^{-27} / 1
Gibbs	-685.88126	-685.93835	35.82	5.31×10^{-27} / 1

3.4.3 Geometry and Bonding in Trimethyl Phosphite

Like other trivalent phosphorus compounds, the phosphorus in trimethyl phosphite has a pyramidal structure. Steric interactions are minimized by orienting one of the alkyl groups in a down or pseudocistoid conformation and the other two in an up or transoid type arrangement. Because of the steric (and perhaps electronic influence of the methyl

groups, the phosphorus and its ligands are more planer in $P(OCH_3)_3$ than in the analogous $P(OH)_3$ molecule. This is indicated by the larger O2-P-O3-O4 dihedral angle (i.e., -100.3° vs. 98°). Each of the three P—O bonds is about 1.6 Å with bond orders about .65 – thereby indicating considerable electron density at the nuclei and less in the bonding region between the two atoms. The P—O—C bond angles are around 120°, thereby suggesting considerable sp^2 character for the oxygens. The geometries, bond orders, and partial charges are listed in Table 13.

Table 13. Geometries, Bonding, and Partial Charges in the B Conformation of Trimethyl Phosphite

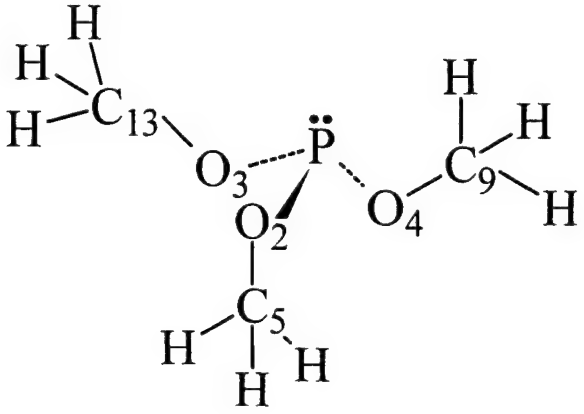

Geometry

Geometric Parameter	AM1	HF/3-21G*	HF/6-31G*	HF/6-311G**
P—O2	1.620	1.598	1.604	1.595
P—O3	1.640	1.630	1.635	1.630
P—O4	1.638	1.618	1.622	1.615
O2—C5	1.408	1.457	1.416	1.417
O3—C13	1.407	1.444	1.407	1.407
O4—C9	1.407	1.444	1.407	1.407
O2-P-O3	99.41	102.01	102.69	102.64
P-O2-C5	114.15	123.43	123.90	125.07
P-O3-C13	111.83	122.32	119.24	120.55
P-O4-C9	108.44	123.52	119.78	121.01
O2-P-O3-O4	-100	-100	-100	-100
O2-P-O3-C13	118	100	91	93
O2-P-O4-C9	-134	158	177	174
O4-P-O3-C13	141	-160	-169	-166
O3-P-O2-C5	53	55	55	55

Table 13 (Continued). Geometries, Bonding, and Partial Charges in the B Conformation of Trimethyl Phosphite

Bond Orders

Bond	AM1	HF/3-21G*	HF/6-31G*	HF/6-311G**
P—O2	.912	.783	.687	.728
P—O3	.871	.663	.632	.675
P—O4	.885	.685	.648	.692
O2—C5	.970	.868	.865	.868
O3—C13	.985	.890	.888	.892
O4—C9	.987	.883	.883	.888

Partial Charges

	AM1	HF/6-31G* CHELP	HF/6-31G* Natural	HF/6-31G* Mulliken
P1	.871	.072	1.770	1.159
O2	-.451	-.276	-.940	-.708
O3	-.470	-.291	-.945	-.744
O4	-.456	-.217	-.938	-.725
C5	-.073	.214	-.228	-.177
C9	-.062	.119	-.228	-.171
C13	-.056	.273	-.229	-.172

All methods indicate that the P-O2 bond (i.e., the cistoid one) is stronger (i.e, has shorter bond length and larger bond order) than the two P—O bonds whose adjacent methyl groups point upward. The corresponding O2—C5 bond is also weaker than the other two. The P-O2-C5 bond angle is also a few degrees larger than the other two.

3.4.4 Vibrational Spectrum of Trimethyl Phosphite

The first vibrational spectrum of trimethyl phosphite was published in 1950.[40] The paper by Meyrick and Thompsom included both infrared and Raman frequencies for 10 small organophosphorus compounds provided by the British Chemical Defense Experimental Establishment at Porton Down. No specific vibrations were assigned to the individual frequencies.

As part of his thesis research at University of Stuttgart, Norbert Fritzowsky recorded the infrared and Raman spectra[41] for $P(OCH_3)_3$, $ClP(OCH_3)_2$, and Cl_2POCH_3 and for the thio analogs.[42] Some very general assignments are included in the paper; however, there was

no detailed analysis of the spectra. Fritzowsky's spectrum as well as that obtained in other laboratories is included in Table 14. The vibrational assignments in the table were based principally on the molecular motions resulting from the Hartree-Fock calculations described above.

Table 14. Empirical Vibrational Spectra of Trimethyl Phosphite

Vapor Aldrich[43]	Liquid Aldrich[44]	Liquid Meyrick[40]	Liquid Fritzowsky[41]	HF/ 6-311G** (Scaled)	Assignment
2954	2947	2990	2991	2925-2868	C—H Stretch (Asym)
		2946	2945		C—H Stretch (Asym)
			2916		C—H Stretch (Asym)
		2902	2895		C—H Stretch (Asym)
2846		2838	2834	2845	C—H stretch(Sym)
1470	1460	1462	1459	1450-1440	C—H Bending (Sizzor)
			1436		
		1265			
1184	1181	1183	1179 1159	1167-1163	C-H Bending (Twisting)
	1113	1121			
1038		1088 1060	1055	1083 1054 1047	P-O-C Stretch
	1012	1014	1012		
760—737	768 730	795 775 738	770 751 731	749 739 708	P—O Stretch
		552	536		
	512	516	513	490	P—O—C Bending
	453 (?)		399	398	P—O—C Bending
			373	365	P—O—C Bending
			283	263	P—O—C Bending
			225	236	P—O—C Bending
			190	180	In-plane deformation
			120	119	Methyl Rotation

The vibrational spectrum of the B conformation of trimethyl phosphite was calculated at the HF/6-31G* and HF/6-311G** levels. A scaling factor of .89 was used to correct for systematic errors resulting from neglect of electron correlation.[45] This molecule contains 16 atoms and therefore 42 vibrational frequencies (i.e., 3N-6). The calculated and scaled frequencies are listed in Table 15. The assignments were made on the basis of frequencies derived from the second derivative of the energy with respect to atomic position and traditional functional group frequencies compiled from numerous empirical measurements.[46] Identification of the specific vibrations was facilitated by visualization of the specific atomic movements with the Gauss View program. Although there is considerable agreement between the calculated assignments and published group frequencies, the assignments in this paper were made independent of literature values.

Table 15. Calculated Vibrational Spectra of Trimethyl Phosphite

Vibration Number	6-31G* (Calc)	6-311G* (Calc)	6-31G* (Scaled)	6-311G** (Scaled)	*Assignment*
42-37	3329-3272	3286-3223	2963-2912	2925-2868	C—H Stretch (Asym)
36	3243	3197	2886	2845	C—H Stretch (Sym, trans)
35-34	3211-3209	3165-3164	2858-2856	2817-2816	C—H Stretch (Sym, cis)
33-28	1662-1650	1630-1618	1479-1469	1450-1440	C—H Bending (Sizzor)
27-26	1635-1633	1609-1608	1455-1453	1432-1431	C—H Bending (wagging, Syn)
25	1626	1601	1447	1425	C—H Bending (wagging, Syn)
24-22	1330-1321	1311-1307	1184-1176	1167-1163	C—H Bending (twisting,Asyn)
21-19	1297-1293	1284-1281	1154-1151	1143-1140	C—H Bending (twisting, Asyn)
18	1221	1217	1087	1083	P-O-C Stretch (Sym)
17	1189	1184	1058	1054	P-O-C Stretch (Asym, cis)
16	1181	1176	1051	1047	P-O-C Stretch (Asym, trans)
15	848	842	755	749	P-O Stretch, cis
14	833	830	741	739	P-O Stretch, trans
13	806	796	717	708	P-O Stretch, cis
12	553	557	492	496	P-O-C Bending
11	443	447	394	398	P-O-C Bending
10	404	410	360	365	P-O-C Bending
9	299	296	266	263	P-O-C Bending
8	265	265	236	236	P-O-C Bending
7	203	202	181	180	In plane deformation
6-2	143-84	141-85	127-75	125-76	Methyl Rotation
1	65	65	58	58	Methyl Rocking

The aliphatic C—H stretching occurs below 3000 cm^{-1}. The absence of a P=O group is evident by the lack of intense vibrations in the 1300-1200 range. Several relatively weak symmetric and asymmetric H-C-H bending vibrations occur in the 1450 cm^{-1} range. In the scissor mode the hydrogens move toward and away from each other simultaneously thereby altering the H-C-H bond angle. In the wagging motions, the hydrogens move in the same direction in a manner resembling rowing a boat. In the twisting motion, the hydrogens move in opposite directions as if the carbon atom was being twisted along its

bond axis. The most intense absorptions occur in the 1040 cm^{-1} range. They result from stretching in the P—O—C group. In this vibration the oxygen moves between the phosphorus and carbon so the P—O bond lengthens as the C—O shortens. In the symmetric mode, all three oxygens move away from the phosphorus simultaneously. In the asymmetric mode, two oxygens move away from the phosphorus while the third moves toward it. Around 750 cm^{-1}, the carbons move away and the oxygens remain relatively stationary. The low frequencies below 600 cm^{-1} are devoted to P—O—C bending and methyl rotation in which all the bond lengths remain essentially constant.

The presence of more than one conformation of trimethyl phosphite may lead to very complex spectra if the analogous vibrations occur at different frequencies. One would surmise that vibrations associated with the methoxy group would be affected more than those involving the P—O bonds only. To test this hypothesis, three vibrations were examined for each of the four conformers. These are listed in Table 16.

Table 16. Effect of Conformation on Calculated Vibrational Frequencies

Conformer	Orientation of methoxy	Vibration 18 (Not scaled)	Vibration 17 (Not scaled)	Vibration 12 (Not scaled)
A	3 up	1233	1187	471
B	2 up; 1 down	1221	1189	553
C	1 up, 2 down	1224	1197	581
D	3 down	1240	1184	601

Vibration 18 is the symmetrical P-O-C stretch in which the three oxygen atoms move away from and toward the phosphorus simultaneously. The range of frequencies is only about 20 cm^{-1}. Vibration 17 is the highest frequency asymmetric P- O-C stretch. The range of frequencies among the conformers is only 10 cm^{-1}. The differences in intensity of absorption may be more dramatic however. When the methyl groups are oriented differently, the P-O stretching can produce different changes in the dipole moment, which will alter the infrared spectrum significantly. In contrast, the orientation of the methoxy should have less impact on the Raman spectrum. Vibration 12 is the symmetrical PO_3 defamation in which the phosphorus moves perpendicular to the plane formed by the three oxygens, increases the O-P-O bond angles, and essentially flattens the structure. The data indicate that the orientations of the alkyl group have considerable influence upon this vibration. The lowest energy vibration at 471 cm^{-1} occurs when the 3 methoxy groups are oriented outward. The frequency increases with the number of methoxy groups oriented downward to a maximal value of 601 cm^{-1}.

3.4.5 Geometric and Electronic Structure of Dimethyl Methylphosphonate

The bond lengths, bond angles, and dihedral angles as well as bond orders and partial charges calculated by various methods for dimethyl methylphosphonate are listed in Table 17.

Table 17. Calculated Parameters for Dimethyl Methylphosphonate

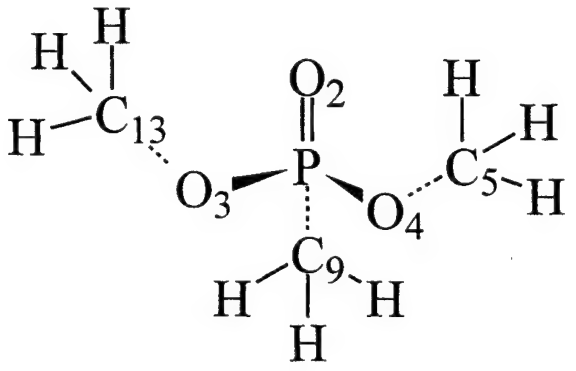

Geometry

	AM1	HF/3-21G*	HF/6-31G*	HF/6-311G**
P—O2	1.458	1.465	1.458	1.453
P—O3	1.614	1.582	1.581	1.573
P—O4	1.613	1.582	1.593	1.586
P—C9	1.630	1.774	1.795	1.789
O3—C13	1.405	1.457	1.419	1.418
O4—C5	1.405	1.457	1.418	1.418
O2-P-O3	111.49	112.83	116.25	116.05
O2-P-O4	111.73	112.83	113.14	112.83
O3-P-C9	120.44	118.92	116.11	116.06
O3-P-O4	101.69	106.35	102.28	102.44
P-O3-C13	118.88	124.29	121.15	122.61
P-O4-C5	115.74	124.32	121.92	123.12
O2-P-O3-O4	-119	-124	-124	-123
O2-P-O3-C13	-18	-24	-49	-50
O2-P-O4-C5	33	24	-25	-25

Table 17 (Continued). Calculated Parameters for Dimethyl Methylphosphonate

Bond Orders

Bond	AM1	HF/3-21G*	HF/6-31G*	HF/6-311G**
P—O2	1.159	1.266	1.173	1.199
P—O3	.634	.681	.659	.700
P—O4	.645	.681	.636	.678
P—C9	.697	.820	.846	.876
O3—C13	.949	.857	.858	.863
O4—C5	.952	.857	.860	.865

Partial Charges

	AM1 Coulson	HF/6-31G* CHELP	HF/6-31G* Natural	HF/6-31G* Mulliken
P	2.687	1.379	2.661	1.537
O2	-1.118	-.765	-1.209	-.732
O3	-.761	-.521	-.942	-.690
O4	-.747	-.518	-.952	-.715
C5	-.042	+.150	-.219	-.178
C9	-.956	-.652	-1.085	-.768
C13	-.036	+.134	-.224	-.187

As would be expected, the P=O2 bond is considerably shorter than the other P—O bonds. The bond order (1.173) is less than twice that for P—O3 (.66) and P—O4 (.64) suggesting greater polarity in the P=O bond than the two P—O bonds. The P—O bonds themselves are very polar with considerable electron density located on the oxygens. The P—C bond is much stronger (.85) than the other phosphorus bonds and is about the same as the two O—C bonds. The bond orders for the two P—O bonds are about the same as for the three P—O bonds in trimethyl phosphite and thereby indicate that the three P—O bonds have little double bond character and the lone pair contributes little to the P—O bonding.

The geometry generated by HF/3-21G* is very symmetrical because the two methoxy groups are almost equivalent with identical bond lengths, angles and opposite dihedrals of 24° and –24°. These dihedral angles create a parallel orientation for the two O—C bonds. In contrast, with the larger 6-31G* and 6-311G** basis sets, the dihedrals have the same sign (i.e., -25° and –50°), which orients the methoxy groups in the same rather than complementary directions. The parallel conformation with HF/3-21G* becomes

a transition structure for the rotation of the methoxy groups in the larger basis sets. The calculated activation barrier for the rotation from one conformer to the other is very small – less than 0.5 kcal/mole.

The orientation around the phosphorus is almost tetrahedral (O2-P-O3-O4 = -123°) with the phosphonyl oxygen occupying slightly more area than the other ligands.

3.4.6 Vibrational Spectrum of Dimethyl Methylphosphonate (DMMP)

The first published infrared and Raman spectra of DMMP appeared in the same article with trimethyl phosphite.[40] The P=O bond is one of the characteristic features of the spectra. Because of the mass of the phosphorus and oxygen atoms, the frequency is less dependent on the size of the substituents; however, changes in electronegativity of the substituents may have significant effects.[47]

Because of the polarity of the P=O bond and the resulting large partial charges on the oxygen (negative) and phosphorus (positive), phosphonates are very susceptible to hydrogen bonding interactions. As a consequence, the stretching vibration of the molecule in the gas phase is different from that in the liquid phase. For example, the P=O stretch of DMMP increases from 1246 cm^{-1} in liquid phase to 1276 cm^{-1} in the gas. Depositing the vapor on an acidic surface such as $FeCl_3$ reduces the bond order of the P=O bond and decreases the frequency to 1173 cm^{-1}.[48]

The most rigorous attempt to assign individual frequencies was made by Van der Veken and Herman in 1981.[49] Prior to this effort they conducted a low level (by today's standard but impressive in 1977) CNDO/2 study and identified 6 stable conformers.[50] The authors were able to identify 51 individual frequencies.[49] They consisted of 28 primary vibrations, 3 overtones, and 20 combination bands. The measured frequencies corresponding to the primary vibrations are listed in Table 18.

The C—H absorptions are in the 2980-2850 cm^{-1} range. The H—C—H bending occurs in the 1400 cm^{-1} range. The C—H stretching and bending vibrations on the methyl carbon are lower frequency than on the methoxy carbon. The P=O stretch, one of the stronger absorptions, occurs around 1260 cm^{-1}. Van der Verken[49] attributed the absorbances at 1058 cm^{-1} and 1032 cm^{-1} to C—O stretching; however, tt seems more likely they result from P—O—C stretches in which the oxygen oscillates between the phosphorus and carbon atoms. In the twisting and rocking motion at 1000 cm^{-1}, the hydrogens twist around or try to invert. This is usually accompanied by some carbon movement also. A medium intensity band at 800 cm^{-1} results from P—C stretching.

Table 18. Empirical Infrared Spectra of the Primary Absorptions of Dimethyl Methylphosphonate Obtained from Various Sources

Aldrich Liquid	Meyrick 40 Liquid	Verken 49 Liquid	Guilbau[48] Liquid	Guilbault [48]Gas	Aldrich Gas	Assignment by Van der Verken[49]
	2990	2995	3000			H—Methoxy (asym)
2956	2946	2955	2960	2960	2964	H—Methyl (asym)
	2902	2930	2935			H – Methoxy (assym)
	2838	2852	2865	2850	2859	H – Methyl (Symm)
			1512			
	1462	1465	1465			H-C-H Bending (Methoxy,Asym)
		1450				H-C-H Bending (Methoxy,Symm)
		1418	1422			H-C-H Bending (Methyl,Asym)
1314		1312	1315	1315	1316	H-C-H Bending (Methyl, Symm)
	1265	1260			1274	P=O Stretch (Conformer 1)
1245		1240	1246	1276		P=O Stretch (Conformer 2)
1185	1183	1185	1186	1185	1187	CH_3-O Rocking
	1121					CH_3-O Rocking
	1060	1058	1060	1076	1047	C—O Stretch (?)
1032	1014	1032	1035	1051		C—O Stretch (?)
915		912	915	920	916	CH_3-P Rocking
		895				CH_3-P Rocking
819		818	820	820	816	O—P—O Stretch
788	795	787	788	792		O—P—O Stretch
	775					
	738	712	714	716	711	P—C Stretch
	552					
501	516	499			500	P-O-C Out of Plane Deformations
		467			463	C-P-O_3 Deformations (Symm)
		411				C-P-O_3 Deformations (Asym)
		398				C-P-O_3 Deformations (Asym)

In previous work, the vibrational spectrum of DMMP was also calculated at the HF/3-21G and HF/6-31G* level using a symmetrical geometry in which one methoxy group was in the trans orientation and the other two were *cis* with O-P-O-C dihedral angles of 29 and –29.[51] The authors compared their calculated frequencies[52] to those measured by Hoffland, Piffath, and Bouck.[53]

In this study, the vibrational spectrum of dimethyl methylphosphonate was calculated by methods identical to those described previously for trimethyl phosphite. The initial guess of the structure of DMMP was optimized with the Berny routine, which is the default routine in Gaussian 98 but was not available in Gaussian 90[51,52] Also, advances in computer hardware allowed more rigorous calculations with the triple zeta quality 6-311G** basis set. The calculated and scaled frequencies obtained with the two basis sets

and the vibrational assignments are listed in Table 19. This molecule is a tautomer of trimethyl phosphite and thereby contains the same number of atoms (16) and primary vibrational modes (42).

Table 19. Calculated Vibrational Spectrum of Dimethyl Methylphosphonate

Vibration Number	6-31G* (Calc)	6-311G** (Calc)	6-31G* (Scaled)	6-311G** (Scaled)	Assignment
42-41	3349-3347	3301-3300	2981-2979	2938-2937	C—H (Asym, Methoxy)
40	3324	3282	2958	2921	C—H (Asym, Methoxy) C—H Stretch, (Asym, Methyl)
39	3319	3272	2954	2912	C—H Stretch (Asym, Methyl) C—H Stretch (Asym, All)
38	3317		2952		C—H Stretch (Asym, Methoxy)
37	3307	3268	2943	2909	C—H Stretch (Asym, Methyl) C—H Stretch (Asym, All)
36	3243	3196	2886	2844	C—H Stretch (Sym, Methoxy)
35	3236	3190	2880	2839	C—H Stretch (Sym, Methoxy) C—H Stretch (Sym, Methyl & Methoxy)
34	3228	3189	2873	2879	C—H Stretch (Sym, Methyl) C—H Stretch (Sym, Methyl & Methoxy)
33-31	1658-1652	1629-1624	1476-1470	1450-1445	C—H Bending, (Sizzor, Methoxy)
30	1650	1619	1469	1441	C—H Bending, (Sizzor, Methoxy)
29-28	1634-1629	1609-1605	1454-1450	1432-1428	C—H Bending, (Wagging, Methoxy)
27-26	1604-1601	1577-1573	1428-1425	1404-1400	C—H Bending, (Sizzor, Methyl)
25	1512	1479	1346	1316	C—H Bending, (Wagging, Methyl)
24	1386	1374	1234	1223	P=O Stretch
23-22	1326-1324	1313-1310	1180-1176	1169-1166	C—H Bending (Twisting)
21-20	1298-1296	1288-1283	1155-1153	1146-1142	C—H Bending (Twisting)
19	1214	1213	1080	1080	P-O-C Stretch (Asym)
18	1183	1181	1053	1051	P-O-C Stretch (Asym)
17	1030	1018	917	906	C—H Bending (Rocking, Methyl)
16	1014	998	902	888	C—H Bending (Rocking, Methyl)
15	889	880	791	783	P—C Stretch
14	865	860	770	765	P—O Stretch
13	773	773	688	688	P—C Stretch & P-O-C Bending
12	539	539	480	480	P-O3 Deformation (Sym)
11	518	519	461	462	P-O3 Deformation (Asym)
10	431	436	384	388	P-O-C Bending
9	320	320	285	385	C-P-O Bending
8	283	287	252	255	C-P-O Bending
7	243	239	216	213	P-O-C Bending
6	197	195	175	174	C-P-O and P-O-C Bending
5	189	193	168	172	Methyl rotation
4	122	118	109	105	Methoxy rotation
3	97	104	86	93	Methoxy rotation
2	77	79	69	70	Methoxy rotation
1	61	65	54	58	Methyl torsional movement

3.5 Phosphite and Phosphonate Tautomers of Bis(2-Ethylhexyl) Phosphonate

3.5.1 Structure Optimization

Bis(2-ethylhexyl) phosphonate contains two long alkyl groups separated by a phosphorus moiety. There is considerable flexibility in the molecule. Although all possible conformations were not examined, considerable effort was expended searching for the global minimum. With the semiempirical methods, the basic structure for the phosphite was optimized, readjusted manually and re-optimized. This structure was converted into the phosphonate by moving the hydrogen. This phosphonate structure was re-optimized. The analogous procedure was performed starting with the phosphonate tautomer. Finally a 15 carbon all trans structure was created with AGUI. The internal carbons were changed to O-P-O group. The structure was optimized after adding the two ethyl groups.

Similar procedures were used for the phosphite tautomer. In addition, the optimized structure of the phosphonate was converted to the phosphite by removing the hydrogen from the phosphorus and adding it to the oxygen. Re-optimization led to additional conformations. The reverse procedure could be used to generate additional phosphonate conformations.

Two or three of the optimized semiempirical structures for each tautomer were used as the input for the ab initio calculations. The all *trans* structure was also used as an additional input geometry. After optimization, frequency calculations confirmed that the optimized structure was an energy minimum and not a transition.

3.5.2 Energies of the Two Tautomers

The energies of the most stable conformer for each tautomer are listed in Table 20. Semiempirical energies are expressed in kcal/mole; whereas ab initio results are in Hartrees. The semiempirical methods indicate that the phosphite tautomer should be the more stable by more than 10 kcal/mole. In contrast, the ab initio results are more consistent with experimentally observed values. At the Hartree-Fock level, both basis sets indicate that the phosphonate tautomer is more stable. The energy difference calculated by HF/3-21G* is 8.72 kcal/mole which translates to a fraction of 4×10^{-7} to one. The energy difference is greater with the HF/6-31G* basis set. The 15.24 kcal/mole energy difference gives a population of only 6.64×10^{-12} to one for the phosphite.

Table 20. Energies and Populations of the Tautomers of *Bis*(2-Ethylhexyl) Phosphonate

Method	Phosphite	Phosphonate	Energy Difference (kcal/mole)	Gas Phase Population Ratio Phosphite/Phosphonate
AM1	-283.45 kcal/mole	-272.81 kcal/mole	(10.64)	$1 / 1.50 \times 10^{-8}$
PM3	-279.22 kcal/mole	-264.27 kcal/mole	(14.95)	$1 / 1.08 \times 10^{-11}$
HF/3-21G*	-1185.3718 (Hartrees)	-1185.3857 (Hartrees)	8.72	$4.02 \times 10^{-7} / 1$
HF/6-31G*	-1191.6285 (Hartrees)	-1191.6528 (Hartrees)	15.24	$6.64 \times 10^{-12} /1$

3.5.3 Structure of the Phosphite Tautomer

With the PM3 semiempirical method, the most stable conformation of the phosphite tautomer is a polar structure having the phosphorus moiety at one end and the alkyl groups at the other. The two hexyl groups were arranged in parallel chains adjacent to each other somewhat similar to a beta sheet protein structure. The ethyl groups were positioned on the outside of the hexyl groups. Even with the input structure configured in the all trans conformation, the molecule reverted to the parallel conformation upon optimization. This parallel geometry can be seen in the dihedral angles. The O3-P-O2-C31 and the O3-P-O5-C6 angles are 50°and –42° respectively. These values are about optimal for initiating two parallel chains from a single point (i.e., the phosphorus atom). The dihedrals at the end of the chain are about 180°. As a result the alkyl chain moves away from the central phosphorus in a zigzag line. The geometries produced by AM1 and HF/3-21G* are the most extended. In each, one of the dihedrals is about 50° and similar to the PM3. The other is about 150° and thereby directs the chain in the opposite direction.

At the HF/6-31G* level, the most stable conformation is V shaped. The O3-P-O2-C31 dihedral at 65° is similar to the PM3 geometry; however the O3-P-O5-C6 is –4° and directs the chain in an acute angle. An open conformation similar to the AM1 was identified at the HF/6-31G* level; however, its energy was 0.3 kcal/mole higher than the V conformation. Some of the geometric and electronic parameters for the most stable conformation of *bis*(2-ethylhexyl) phosphite are listed in Table 21. In the illustration of the structure, the hydrogens were omitted for clarity.

Table 21. Geometric and Electronic Structure of *Bis*(2-Ethylhexyl) Phosphite

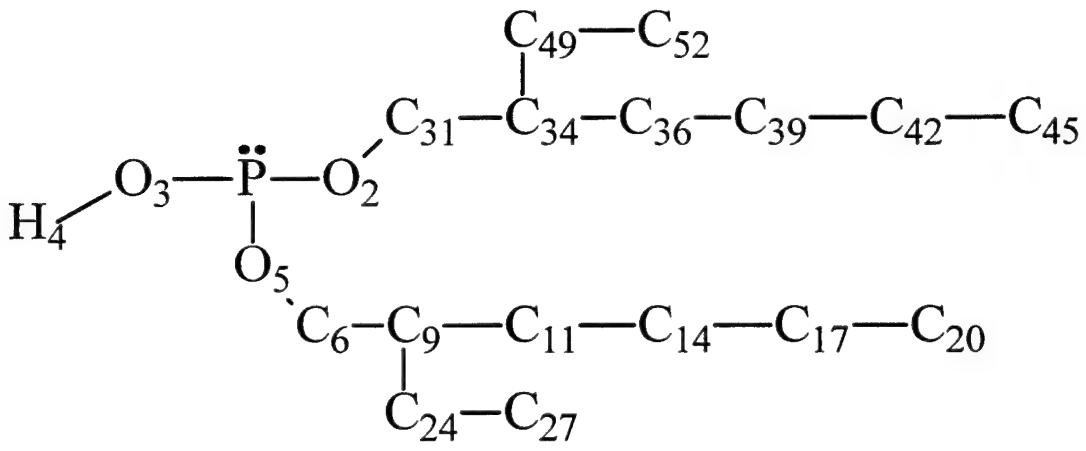

Geometry

Parameter	AM1	PM3	HF/3-21G*	HF/6-31G*
P—O2	1.62	1.70	1.631	1.620
P—O3	1.62	1.68	1.621	1.632
P—O5	1.63	1.71	1.609	1.630
O2—C31	1.41	1.39	1.451	1.412
O5—C6	1.41	1.39	1.456	1.412
O3—H4	.96	.94	.968	.949
C31—C34	1.53	1.55	1.532	1.526
C34—C36	1.52	1.53	1.546	1.538
C34—C49	1.52	1.53	1.550	1.546
C36—C39	1.51	1.52	1.540	1.530
C39—C42	1.51	1.52	1.540	1.530
C42—C45	1.51	1.51	1.540	1.528
C49—C52	1.51		1.541	1.530
P-O2-C31	118.1	127.4	123.87	126.95
P-O5-C6	113.4	127.5	126.02	128.46
P-O3-H4	110.6	122.3	118.39	117.51
O2-P-O5	99.5	104.7	100.02	101.10
O2-C31-C34	110.8	111.1	112.12	109.22
O5-C6-C9	110.4	111.4	109.94	110.16
C31-C34-C49	110.5	108.2	110.90	111.00
C31-C34-C36	107.8	110.0	107.89	108.6
O3-P-O2-O5	96	107	103.7	104.6
O3-P-O2-C31	50	50	-152.6	65.3
O3-P-O5-C6	151	-42	-52.8	-3.8
P-O2-C31-C34	16	129	91.4	-117.2

Table 21 (Continued). Geometric and Electronic Structure of *Bis*(2-Ethylhexyl) Phosphite

P-O5-C6-C9	-121	-131	133.85	169.9
O2-C31-C34-C36	141	-162	174.8	-171.2
O2-C31-C34-C49	60	73	51.9	63.0
C31-C34-C36-C39	173	162	1563.5	174.4
C34-C36-C39-C42	-174	174	179.1	-137.3
C36-C39-C42-C45	-179	-178	179.3	-175.9
C36-C39-C42-C45	-139	-150	-94.1	-179.6

Bond Order

	AM1	PM3	HF/3-21G*	HF/6-31G*
P—O2	.87	.81	.663	.657
P—O3	.91	.86	.705	.664
P—O5	.85	.81	.717	.636
O2—C31	.96	.97	.867	.863
O5—C6	.96	.97	.859	.861
O3—H4	.92	.91	.744	.731
C31—C34	.96	.96	.998	1.001
C34—C36	.98	.98	.994	1.003
C34—C49	.98	.98	.991	.993
C36—C39	.99	.99	.927	1.013
C39—C42	.99	.99	1.007	1.013
C42—C45	1.00	1.00	1.016	1.024
C49—C52	1.00	1.00	1.016	1.024

Partial Charges

Atom	AM1 Coulson	PM3 Coulson	HF/6-31G* CHELP	HF/6-31G* Natural	HF/6-31G* Mulliken
P	.97	1.23	.118	1.799	1.226
O2	-.48	-.56	-.261	-.950	-.740
O3	-.53	-.60	-452	-1.089	-.860
H4	.23	.21	.348	.497	.456
O5	-.52	-.56	-.143	-.964	-.775
C31	.00	.11	.118	-.016	.009
C34	-.12	-.11	.184	-.250	-.162
C36	-.15	-.11	-.186	-.423	-.319
C39	-.15	-.13	.151	-.420	-.306
C42	-.16	-.11	.044	-.420	-.303
C45	-.21	-.12	-.178	-.631	-.479
C49	-.15	-.09	-.189	-.423	-.323
C52	-.21	-.12	.050	-.627	-.485

The P—O bond lengths for each of the 3 bonds are about 1.6 Ă with all methods. There isn't any consistent difference in bond lengths. The P—O bonds are about 1.4 Ă. The HF/3-21G* values are slightly longer. The P—O—R bonds are in the 110° to 120° range. With all methods that P—O—H bond angle is smaller than the two P—O—C bonds. AM1 values are smallest and thereby indicate more p character. The effect of the overall geometry is reflected in the bond angles. The PM3 structure has the most overall symmetry and almost identical bond angles. The V shaped HF/6-31G* structure is also reasonably symmetrical. In contrast the alkyl groups in the AM1 structure are different and contribute to bond angles differences of 5°. As was seen in the trimethyl phosphite, the lone pair on the phosphorus occupies considerable space and thereby forces the alkoxy substituents into a smaller space. The extent of the crowing can be seen in the dihedral describing the tetrahedral nature around the phosphorus. The O3-P-O2-O5 of 96 to 107 degrees is considerably less than the value of 120° for a regular tetrahedron.

The semiempirical bond orders for the P—O bonds are slightly larger than the HF/3-21G* which is slightly larger than the HF/6-31G* value. The bond orders for the P—OH bond are slightly larger than the P—OC bonds; however, the difference is not large. The O—C and C—C bonds approach unity. As is usually seen, the bond orders for the terminal C—C bonds are slightly larger (.01 unit) than the internal ones. The C—C bonds adjacent to the oxygens are the weakest.

The absolute values of the partial charges depend on the method used to calculate them and to some extent the basis set. All indicate excess positive charge on the phosphorus and excess negative charge on the oxygens and most of the carbons. The charge on the carbon atoms is essentially a function of the number of hydrogens.

3.5.4 Structure of Bis(2-Ethylhexyl) Phosphonate (Phosphonate Tautomer)

Like the phosphite tautomer, the most stable conformation of *bis*(2-ethylhexyl) phosphonate depended on the method. Both AM1 and PM3 generated the parallel structure similar to that described for the phosphite tautomer. In this structure, the carbon atoms at the ends of the hexyl chains were 3.9 Å apart. With AM1, the energy of a partially open conformation was about 3 kcal/mole higher than the parallel conformation. The most stable HF/3-21G* structure was V type with the carbon ends about 8 Å apart. Among the various computational methods, HF/6-31G* produced the most open most open or extended structure. In this conformation, the two terminal carbon atoms were separated about 14 Å.

The geometric parameters for the most stable conformation with each method are included in the top section of Table 22. The bond orders calculated by semiempirical methods and the Wiberg bond indices for the ab initio methods constitute the middle section. In the bottom section, the Coulson charges from the AM1 and PM3 methods along with the CHELP, Natural Bond Order, and Mulliken charges from the HF/6-31G* calculation. The hydrogen atoms in the structure have been eliminated for clarity.

Table 22. Geometric and Electronic Structure of *Bis*(2-Ethylhexyl) Phosphonate

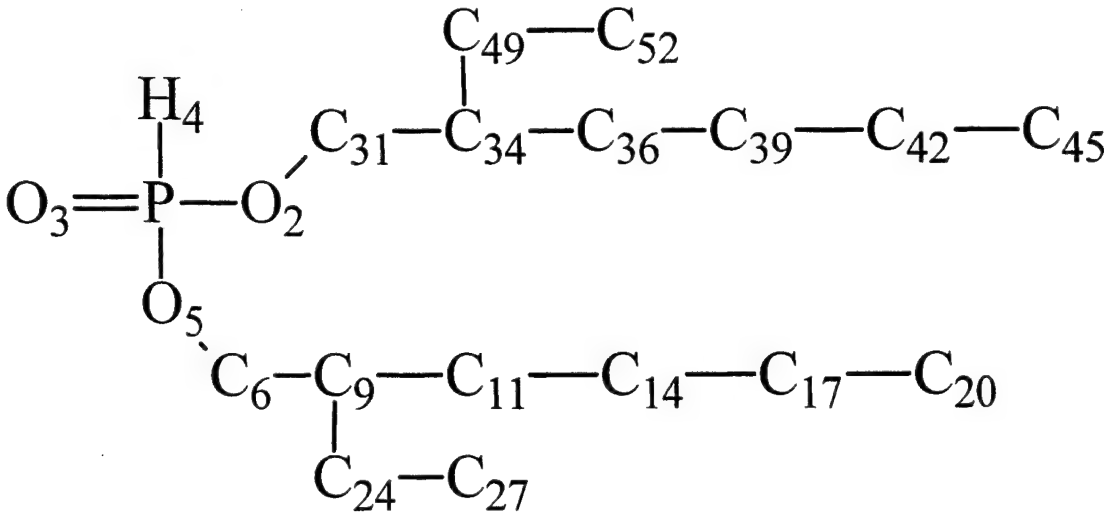

Geometry

Parameter	AM1	PM3	HF/3-21G*	HF/6-31G*
P-O2	1.60	1.72	1.582	1.573
P-O3	1.46	1.46	1.460	1.454
P-O5	1.60	1.72	1.570	1.585
P-H4	1.28	1.23	1.372	1.377
O2—C31	1.41	1.40	1.471	1.431
O5—C6	1.41	1.40	1.471	1.428
C31—C34	1.53	1.55	1.528	1.524
C34—C36	1.52	1.53	1.545	1.538
C34—C49	1.52	1.53	1.549	1.546
C36—C39	1.51	1.52	1.540	1.530
C39—C42	1.51	1.52	1.541	1.530
C42—C45	1.51	1.51	1.540	1.528
C49—C52	1.51	1.51	1.542	1.530
H4-P-O2	102.6	101.3	104.61	99.99
H4-P-O3	119.8	124.4	116.80	115.27
H4-P-O5	102.1	101.6	100.14	104.92
P-O2-C31	119.1	120.5	124.03	122.19
P-O5-C6	118.7	120.6	123.75	121.94
O2-P-O5	104.1	102.5	109.04	102.57
O2-C31-C34	110.9	110.1	111.48	108.78
O5-C6-C9	110.2	110.6	111.48	110.03
O3-P-O2-O5	123	120	127.0	126.5
O3-P-O2-C31	10	46	-24.2	51.5

Table 22 (Continued). Geometric and Electronic Structure of *Bis*(2-Ethylhexyl) Phosphonate

O3-P-O5-C6	-23	-39	-41.5	32.8
P-O2-C31-C34	117	146	144.7	-169.0
P-O5-C6-C9	-120	-143	-89.0	-170.7
O2-C31-C34-C49	62	83	59.0	63.9
O2-C31-C34-C36	-174	-153.6	-177.0	-170.55
C34-C36-C39-C42	-172	175.3	-174.8	-176.04
C36-C39-C42-C45	180	-179.8	-179.5	-179.65

Bond Order

Bond	AM1	PM3	HF/3-21G*	HF/6-31G*
P-O2	.67	.64	.670	.636
P-O3	1.17	1.29	1.323	1.224
P-O5	.67	.64	.671	.636
P-H4	.69	.79	.886	.910
O2—C31	.93	.97	.880	.870
O5—C6	.93	.97	.878	.869
C31—C34	.96	.97	.991	.994
C34—C36	.98	.98	1.000	1.001
C34—C49	.98	.98	.995	.998
C36—C39	.99	.99	1.009	1.014
C39—C42	.99	.99	1.008	1.014
C42—C45	1.00	1.00	1.020	1.027
C49—C52	1.00	1.00	1.020	1.027

Partial Charges

	AM1 Coulson	PM3 Coulson	HF/6-31G* CHELP	HF/6-31G* Natural	HF/6-31G* Mulliken
P	2.60	2.17	1.309	2.418	1.519
O2	-.74	-.66	-.630	-.933	-.767
O3	-.109	-.91	-.720	-1.165	-.707
H4	-.46	.25	-.006	-.125	-.014
O5	-.74	-.66	-.653	-.933	-.768
C31	.01	.13	.341	-.005	.015
C34	-.12	-.10	-.017	-.263	-.158
C36	-.15	-.11	-.041	-.420	-.321
C39	-.16	-.11	.016	-.421	-.305
C42	-.16	-.11	.205	-.420	-.302
C45	-.21	-.11	-.267	-.634	-.477
C49	-.15	-.09	.154	-.435	-.311
C52	-.21	-.12	-.218	-.628	-.481

As would be expected, the P=O bonds are shorter than the two P—O bonds. In the parallel structures (AM1 and PM3), the two P—O bonds have the same length. The bond lengths are slightly different in the asymmetrical ab initio structures. As was seen in the other phosphonates, the phosphonyl oxygen occupies more space than the other phosphorus ligands. This feature can be seen in the three H-P-O bond angles and the small O2-P-O5 bond angle of 100°. The P-O-C bond angles are about 120° and are consistent with sp^2 hybridization.

The bond order for the P=O bond is about 1.2. This value indicates very little double bond character. The electron distribution in this part of the molecule is partitioned away from the phosphorus and toward the more electronegative oxygens. With the Mulliken method, the charge on the phosphonyl oxygen is less than on the other two oxygens. With the CHELP method, the phosphonyl oxygen has greater electron density than the other two oxygens. The charge on the phosphonyl hydrogen is near zero but negative. Typical values for hydrogen bonded to carbon are about .15 with Mulliken and .03 with CHELP. The hydrogen is drawing considerable electron density from the phosphorus. The P—H bond has the highest bond order of the single bonds and the hydrogen has slightly excess charge.

3.5.5 Vibrational Spectrum of Bis(2-Ethylhexyl) Phosphonate

The vibrational frequencies of *bis(*2-ethylhexyl) phosphonate obtained by FT-IR are listed in Table 23 with the frequencies calculated at the HF/6-31G* level. The molecular motions corresponding to frequencies are tabulated in the right column. *bis(*2-ethylhexyl) phosphonate contains 159 vibrational modes in addition to the 3 rotational and 3 transitional. Some of the frequencies such as P—H stretching are unique; however, the large number of C—C and C—H bonds generates many stretching, bending and rocking motions that have almost the same energy. Therefore many of these are grouped together in Table 23. Some of the C—H bending frequencies extend through the P=O region so that some absorptions result from very complicated atomic movements. As was done with the other two spectra, the calculated frequencies were scaled by .89 to minimize systematic errors arising from the absence of electron correlation in the calculations.[45]

Table 23. Vibrational Spectrum of *Bis*(2-Ethylhexyl) Phosphonate

Vibration Number	HF/6-31G* (Calculated)	HF/6-31G* (Scaled)	Infrared Coblenz Ref 54	Infrared Aldrich) Ref 55	Inten	Assignment
159-145	3311-3233	2947-2877	2940	2960	S	C—H Stretch Asym,
144-143	3213-3211	2860-2858				C—H Stretch, Symm
142-140	3212-3205	2859-2852				C—H Stretch, Asym
139-134	3205-3198	2852-2846				C—H Stretch, Symm
133	3194	2843				C—H Stretch, Asym & Sym
132-126	3193-3175	1842-2826				C—H Stretch, Symm
125	2785	2479	2440	2440	W	P—H Stretch

Table 23 (Continued). Vibrational Spectrum of *Bis*(2-Ethylhexyl) Phosphonate

124-107	1674-1671	1490-1487	1470	1463	S	C—H Bending (Sizzor)
106-98	1584-1552	1410-1381	1390	1380	M	C—H Bending (Wagging)
97	1548	1378				C—H Bending (Twisting)
96-95	1525-1524	1357-1356				C—H Bending (Wagging)
94-85	1491-1420	1327-1264				C—H Bending (Twisting)
84	1405	1250	1270	1262	S	P=O Stretch
83	1402	1248				C—H Bending (Twist and Wag)
82	1398	1244				P=O Stretch
81-78	1391-1355	1238-1206				C—H Bending (Twisting)
77-74	1299-1268	1156-1129	1150	1150	W	C—H Bending
73-72	1255-1244	1117-1107				C—C Stretch
71	1236	1104		1113	W	P-O-C Stretch (Symm)
70	1195	1064	1040	1040	S	P-O-C Stretch (Asym)
69	1084	965				C-H Bending (Wagging)
68	1178	1048				P-O-C Stretch (Asym)
67-66	1157-1149	1030-1023				Twisting
65-64	1142-1140	1016-1015				C—C Stretch
63	1136	1011				P-O-C Stretch
62-61	1121-1112	998-989				C—C Stretch
60	1103	982				P-O-C Stretch
59	1094	974				C—C Stretch
58-57	1084-1080	965-961	980	976	S	P-O-C Stretch
56-54	1067-1055	950-939				C—C Stretch
53-52	1009-1008	898-897				Rocking and Twisting
51-50	971-969	864-862				C—C Stretch
49	950	846	860	863	M	P—O Stretch, Asym
48	911	811	780	780	W	P—O Stretch Symm
47-40	896-785	797-699		730	W	CH_2 Rocking
39	629	560		543	W	PO_3 Deformation, Symm
38-35	579-524	515-466				C-C-C Bending
34	477	425				O-P=O Bending + other
33	453	403				O-P-O Bending
32	445	396				C-C-C Bending
31	422	376				O-P-O Bending
30-26	351-291	312-259				C-C-C Bending
25-21	274-235	244-209				Methyl rotation
20-16	231-162	206-144				Skeleton Movement caused by C—C rotation
15	154	137				C-C-C, P-O-C Bending
14-1	140-8	125-7				Skeleton Movement caused by C—C rotation

As is typical for sp^3 carbons, all C—H stretching frequencies occur below 3000 cm^{-1}. In general the asymmetric C—H vibrations (one C-H lengthens while the other contracts) are higher frequencies than the symmetric ones. Also C—H stretching in the methylene (CH_2) groups is higher frequency than the terminal methyl (CH_3) vibrations; however, the molecule contains 34 hydrogen atoms so the vibrational motion is quite complex. The most characteristic vibration is the P—H stretch. This weakly absorbing frequency at 2440 occurs in a relatively open part of the spectrum and is usually not mislabeled except

for occasional overtones or combination bands. The 51 C—H bending vibrations consume considerable parts of the spectrum from 1500 to 1100 cm^{-1}. Many of these vibrations overlap with intense absorbances. Among the C—H bending motions, the scissor vibration around 1465 cm^{-1} has the highest frequency. In this vibration, the hydrogens move toward each other in a scissor manner. The C—H wagging vibrations occur around 1400 cm^{-1}. In this vibration, the hydrogens move in the same direction along the C—C bond axis. The methyl wag is very dramatic with the CH_3 group essentially inverting. Most of the twisting vibrations were too weak to be reported. The very strong P=O stretch occurs in the 1265 cm^{-1} range. In the calculated spectrum, the P=O stretch exists as a doublet with frequencies at 1250 and 1244 cm^{-1}. It is reasonable that this intense absorbance was not resolved in the spectrum of the neat liquid. The splitting of the P=O into a doublet is common and frequently attributed to Fermi resonance.[47] The symmetric P-O-C stretch is weakly absorbing at 1113 cm^{-1}. This vibration is weakly absorbing in the infrared because the oxygen atoms move radially from the phosphorus and thereby don't change the dipole moment appreciably. In contrast, this vibration gives an intense Raman band due to the change in the electron density around the phosphorus (and oxygens). In contrast, the asymmetric P-O-C stretches are very intense. The frequencies at 1040 and 976 cm^{-1} result from the movement of the oxygen between the phosphorus and nitrogen. During this vibration the O-P-H bond angle changes dramatically due to movement of the hydrogen. Also, there is considerable movement of the carbon atoms located near carbon 1. In the P—O stretch at 863 cm^{-1}, the O—C bond length does not change much. The movement of the oxygen in the center of the molecule is accommodated by change in the O-C-C bond angle. The weak absorbance at 730 cm^{-1} results from a CH_2 rocking motion. Both hydrogens move in the same direction. This vibration is more of a twisting of the C—C bond than an H-C-H bending mode and accounts for its low energy. The PO_3 symmetrical deformation is a low intensity peak at 543 cm^{-1}. In this vibration, the phosphorus and the phosphonyl oxygen move toward the center of the other three oxygens as they move outward. The O-P-O bond angles change; however, there is no change in the P-O bond lengths. The calculated spectrum contains several low energy vibrations whose frequencies are less than measurable by many spectrometers. Various C-C-C and O-P-C bending modes occur in the 500 to 300 cm^{-1} range. The lowest frequency vibrations are rotations about C—C bonds such as methyl groups and larger fragments.

4. DISCUSSION

The initial calculations on a series of phosphorus halides provided a comparison between trivalent and tetravalent phosphorus compounds. These were followed by calculations on selected phosphorus acids to gain some insight into electronic aspects related to tautomerization of phosphorus compounds and the effect of a P—H bond on the system. The third series contrasted the trimethyl phosphite and its stable tautomer dimethyl methylphosphonate. Extensive calculations were performed on this series because some thermochemical data was available for comparison. The results from these studies were

used to select the most appropriate levels of theory and basis sets for calculations on *bis*(2-ethylhexyl) phosphonate (BIS).

Semiempirical methods are useful in determining the geometry and bonding parameters for molecules containing atoms that have been accurately parameterized. The truncated Hartree-Fock Hamiltonian allows rapid calculations on molecules too large for higher levels of theory but frequently fails when a precise energy calculation is critical. Sometimes, as a result of parameterization, energy calculations are accurate to within 0.5 kcal/mole; however, such isolated results are essentially fortuitous and have little predictive value. As a general rule, except for similar or closely related systems, 5 kcal/mole is the limit of the accuracy of energy calculations using semiempirical methods. A difference of 5 kcal/mole between species in equilibrium translates into a population ration of $1 / 2 \times 10^4$ at 298° K based on a Boltzman distribution.

As would be expected, all methods generated accurate geometries for PCl_3 and $POCl_3$. These molecules have been studied with various experimental techniques. Undoubtedly PCl_3 and probably $POCl_3$ were used in the parameterization of AM1 and PM3. It is somewhat interesting that optimization with MP2/6-31G* produced bond lengths and angles that differed from experimental more than the HF/6-31G* values. This is somewhat disturbing because single point MP2, MP3, and MP4 energy calculations are frequently performed on Hartree-Fock generated geometries. If the single point calculations are performed on unstable structures, then by definition, the energy calculation is not the lowest that could be obtained at that level of theory.

In this study, both AM1 and PM3 methods favored the phosphite tautomer over the phosphonate. The calculations indicated that phosphorus acid, $P(OH)_3$ would be more abundant than phosphonic acid, $HPO(OH)_2$. Similarly, both methods predicted that the phosphite tautomer of *bis*(2-ethylhexyl) phosphonate (BIS) would be more stable than the phosphonate tautomer. For phosphonate systems that don't contain a P—H bond such as trimethyl phosphite / dimethyl methylphosphonate, the equilibrium lies so far toward the pentavalent structure, that the semiempirical result is qualitatively correct. Quantitatively, the semiempirical results were similar to the other systems. In the three phosphonates studied, the energy differences calculated by HF/6-31G* was about 30 kcal/mole greater than with PM3.

In contrast, ab initio methods, even those with the small 3-21G* basis set, correctly predicted that the phosphonate tautomer would have lower energy. A few test calculations were performed on small molecules with the triple zeta quality 6-311G** basis set. This basis set contains polarization functions for hydrogen in addition to the heavy atoms. Because the results from these calculations were similar to those at the HF/6-31G* level there seemed to be no reason for using the more rigorous and more costly methods with the larger molecules.

If the phosphorus compound has sufficient electron withdrawing groups, the equilibrium can shift toward the phosphite form. It has been demonstrated experimentally, that the equilibrium of *bis*(trifluoromethyl) phosphorus acid lies toward the trivalent species; however, the energy difference (and the resulting population ratio) has not been

measured. Both semiempirical methods and ab initio calculations with HF/3-21G* and the HF/6-31G* indicated the trivalent species would have lower energy. The HF/6-31G* was 6.65 kcal/mole, which translates to a population of 1×10^{-5} to one for the pentavalent species.

The result of energy calculations in Gaussian 98 is the total energy of the system expressed in atomic units or Hartrees. One Hartree equals 627.5 kcal/mole. The free energy is the energy that is available for chemical reactions and equals the total energy minus the unavailable energy. The unavailable energy is the product of the temperature and entropy, which is a measure of the randomness in the system among other things. It is possible that the entropy for the phosphite tautomer with three bonds to phosphorus might be systematically different from the entropy of the phosphonate with four ligands. To obviate this potential source of error, entropy calculations were performed on each of the optimized structures. A value of $298 \times \Delta S$ was subtracted from the total energy to give the Gibbs free energy. This entire calculation was performed by the Gaussian 98 program as part of the overall frequency subroutine. Removing the entropy contribution from the overall energy altered the energy and the population slightly – less than a kcal.

Density functional methods have recently become popular because they generate reasonably accurate results (frequently more accurate than Hartree-Fock calculations at the same level of theory) with less computer time. The hybrid functional 3BLYP/6-31G* was used to calculate the energies of $P(OMe)_3$ and $MeP(O)(OMe)_2$. The energy difference between the two tautomers was 25.5 kcal/mole, which was the smallest value generated by the non-semiempirical methods.

Compound calculation methods using a sequence of calculations having different levels of rigor have been developed to generate more accurate results with less computational time. The G1[35] and G2[36] methods arrived in the early 1990's. The CBS system was published in the mid 1990's. Trimethyl phosphite and dimethyl methylphosphonate were studied at the CBS-Q level.[37] The energy differences (internal energy, enthalpy, and Gibbs free energy) between the tautomers was about 36 kcal/mole, which was the largest difference among all methods.

The accuracy obtained with high level calculations on hydrocarbons and similar compounds is not achieved with compounds containing phosphorus. The reason for the difficulty is not apparent. Lack of empirical thermodynamic data on phosphorus compounds and the inability of ab initio methods to calculate thermodynamic properties with sufficient precision led to the development and introduction of empirical corrections into ab intio results. Using the Bond Additivity Correction method, Glaube *et al* were able to obtain the empirical heat of formation for dimethyl methylphosphonate to within 0.1 kcal/mole.[9] The BAC-4 method adds the following correction terms to the MP4 result:[56]

1. individual atom term
2. molecular term
3. individual bond term

This approach has recently been modified to use G2 results and applied to inorganic compounds such as aluminum.[57] The utility of this approach will depend on generality of the empirically derived parameters.

It is important to remember that the thermodynamic properties are relevant to the chemical equilibrium in a system and are unrelated to the rate at which equilibrium is achieved. The kinetics depend principally on the height of the reaction barrier or energy of activation. These values are unrelated to the rate with which equilibrium may be achieved when one of the tautomers is added to solution. The rate is determined by the energy difference between the reactant and the transition structure that separates the two tautomers. This value is usually called the energy of activation. For hydrogen phosphonates or other compounds having a H—P=O group, the interconversion may be fairly rapid due to acid/base catalysis so reactions involving only one of the tautomers may proceed expeditiously. For compounds like trimethyl phosphite, which have no P—H or P—OH groups, the interconversion may be very slow.

The geometries optimized by semiempirical methods usually had identical bond lengths and angles and opposite dihedral angles that produced a symmetrical molecule – frequently with a plane of reflection but sometimes with C_{3v} symmetry forming a propeller type geometry. In contrast, at the higher levels of theory, the substituents were arranged to maximize separation so that both substituents would go to the left or both to the right – thereby forming an asymmetric structure.

The central phosphorus atom in the phosphites contains three ligands in a trigonal configuration with a lone pair of electrons at the apex. The O—P—O bond angles were 99.4 degrees with AM1 and about 102° with the three ab initio basis sets. Because a tetrahedral arrangement would have 109.5° angles, the three ligands are crowded on one side of the molecule by the lone pair. In trimethyl phosphite, the P—O—Me bond angle is about 120°. Depending on the dihedral angles, the methyl group may be oriented up on the side of the molecule with the phosphorus lone pair, may be oriented down away from the lone pair, or may be oriented horizontally somewhere near the plane created by the three oxygens. Calculations indicated that the most stable conformation (lowest energy) has one methyl oriented down and two somewhat up. One is more up than the other. This arrangement permits good separation of the methyl groups.

The P—O bond order is greater when the methyl group is oriented down. The bond order is least when the methyl points up and intermediate when the methyl is in the equatorial position. This phenomenon may help explain why the propeller conformation (all methyls up) is one of the least stable even though there is minimal steric crowding. It is reasonable that the methoxy with the smallest bond order would be the most reactive. The slight preference could also be magnified by the phosphorus lone pair located in the vicinity.

The equilibrium for *bis*(2-ethylhexyl) phosphonate is sufficiently toward the phosphonate that the infrared spectrum contains no evidence of the phosphite isomer. The calculated ratio of 10^{-12} also indicates that only traces of the phosphite would be present. The

concentration of phosphite is much greater than the equilibrium concentration of trimethyl phosphite/dimethyl methylphosphonate (10^{-22}). Nevertheless it should be possible to run reactions specific for the phosphite — especially in a basic environment that would abstract the proton and accelerate the tautomerization.

The calculations on BIS were performed on the isolated molecule. In the most stable conformation, the phosphorus group was on one side of the molecule and the both hydrocarbon chains were on the other. The degree of opening, i.e., whether the chains were parallel or V shaped depended on the level of theory – parallel at low levels and V at the higher. As would be expected, the difference between conformers was not great so considerable populations of different conformers probably exist in condensed phases. At the HF/6-31G* level, the P=O and P—O bond orders were slightly greater than the corresponding bonds in DMMP. The P—H bond in BIS (.86) was slightly less that the P—H bond in phosphonic acid (.89).

In general, the partial charges from the natural bond order method had the greatest magnitude. CHELP charges were the smallest. For example the CHELP partial charge on phosphorus in BIS (phosphite tautomer) was 0.18 in contrast to 1.80 with Natural and 1.23 with Mulliken.

It appears that the presence of a hydrogen atom attached directly to the phosphorus reduces the energy difference between the phosphite and phosphonate tautomer. For the compounds studied, the shift was not sufficient to shift the equilibrium to a position in which the phosphite predominated.

The most important aspect of the frequency calculations is not exact reproduction of the vibrational spectrum but identification of the individual vibrations and matching them to the frequencies. Frequency calculations at the HF/6-31G* level are reasonably accurate if the .89 correction factor is included. Because BIS contains 159 vibrational modes, there will be considerable overlap in the empirical spectrum. In the C—H stretching region around 3000 cm^{-1}, only 2 absorption maxima are identified in the Aldrich spectrum; however, 34 were present in the calculated spectrum. Unique absorbances are easier to evaluate. Calculated P—H stretch at 2479 cm^{-1} corresponds to the empirical 2440 cm^{-1}.

For simulant applications, the most relevant vibrations are those involving the phosphorus oxygen bonds. They normally have intense absorbencies, are present in the OP nerve agents, and are reasonably independent of structure. The calculated P=O stretch for BIS occurs at 1250 and 1244 cm^{-1} in comparison with 1270 (Coblenz) and 1262 (Aldrich). The single bond stretching occurs at two locations in the spectrum. The symmetrical stretching in which the oxygen remains stationary occurs at 1100 cm^{-1} (calculated). The asymmetric stretching, in which the phosphorus and carbon remain essentially stationary and the oxygen moves between them, occurs at 1062 (calculated). The corresponding values for DMMP are 1080 and 1053 cm^{-1} respectively. The corresponding empirical values are 1040 for BIS and 1048 cm^{-1} for DMMP. The

frequencies for the other P—O are more variable. They occur in the 960-980 cm^{-1} range for BIS and 687 cm^{-1} for DMMP.

5. SUMMARY

None of the methods examined, i.e., semiempirical, ab initio at the Hartree-Fock or Møller-Plesset, density functional, or compound methods, produced energies consistently within 5 kcal/mole of empirical values. Semiempirical methods frequently predicted that the wrong tautomer would be the more stable. In contrast, ab initio methods predicted the correct tautomer even with small basis sets.

For phosphite-phosphonate systems, the equilibrium lies toward the phosphonate tautomer unless there are sufficient electron withdrawing groups attached to the phosphorus to alter the equilibrium. The presence of hydrogen atoms directly attached to phosphorus reduces the energy difference between the tautomers and thereby increases the concentration of the minor tautomer.

The calculated vibrational spectra for trimethyl phosphite, dimethyl methylphosphonate and *bis*(2-ethylhexyl) phosphonate (BIS) agree reasonably well with empirical spectra.

LITERATURE CITED

(1) Deiner, Albert; Johnson, William C.; Koblin, Abraham "The Selection of Bis(2-Ethylhexyl) Hydrogen Phosphite as a V-Agent Simulant, and the Development of Analytical and Field Sampling Techniques for its Use (U)," Army Chemical Center; CWLR 2215, April 1958, Declassified on 28 Sept 1964.

(2) Sass, Samuel; Cassidy, James; "Colorimetric Estimation of Dialkyl Phosphites in Presence of Trialkyl Phosphites, Phosphates, and Phosphonates;" *Analytical Chemistry*, vol 28, p 1968-70 (1956).

(3) Quin, Louis D., "The P--OH to P(O)H Rearrangement with 3-Coordinate Phosphorus" in *A Guide to Organophosphorus Chemistry*; Wiley Interscience: New York, 2000; pp 20.

(4) Guthrie, J. Peter; Cullimore, Particia A.; "The Enol Content of Simple Carbonyl Compounds: A Thermodynamic Approach;" *Canadian Journal of Chemistry*, vol 57, p 240 (1979).

(5) Martin, R. Bruce; "The Rate of Exchange of the Phosphorus Bonded Hydrogen in Phosphorus Acid;" *Journal of the American Chemical Society*, vol 81, p 1574-76 (1958).

(6) Corbridge, D.E.C., in *Phosphorus: An Outline of Its Chemistry, Biochemistry, and Uses*; 5th ed.; Elsevier: Amsterdam, 1995; p 247.

(7) Lewis, Edward S.; L. Gene Spears, Jr.; "Ionization of the PH bond in Diethyl Phosphonate;" *Journal of the American Chemical Society*, vol 107, p 3918-21 (1985).

(8) Guthrie, J. Peter; "Tautomerization Equilibria for Phosphorus Acid and its Ethyl Esters, Free Energies of Formation of Phosphorus and Phosphonic Acids and their Esters, and pKa Values for Ionization of the P--H Bond in Phosphonic Acid and Phosphonic Esters;" *Canadian Journal of Chemistry*, vol 57, p 236-9 (1979).

(9) Glaude, P.A.; Curran, H.J.; Pitz, W.J.; Westbrook, C.K.; "Kinetic Study of the Combustion of Organophosphorus Compounds;" *Proceedings of the Combustion Institute*, 28(Pt. 2), 1749-1756 (2000).

(10) Dean, John A.; "Table 6.1 Enthalpies and Gibbs Energies of Formation, Entropies, and Heat Capacities" in *Lang's Handbook of Chemistry*; 14th ed.; McGraw-Hill: New York, 1992; p 6.39.

(11) "AMPAC 6.55," Semichem Inc, Shawnee, KS; (1999).

(12) Frisch, M.J.; Trucks, G.W.; Schlegal, H.B.; Scuseria, G.E.; Robb, M.A.; Cheeseman, J.R.; Zakrzewski, V. G.; J.A. Montgomery, Jr.; Stratmann, R.E.; Burant, J.C.; Dapprich, S.; Millam, J.M.; Daniels, A.D.; Kudin, K.N.; Strain, M.C.; Farkas, O.; Tomasi, J.; Barone, V.; Cossi, M.; Cammi, R.; Mennucci, B.; Pomelli, C.; Adamo, C.; Clifford, S.; Ochterski, J.; Petersson, G.A.; Ayala, P.Y.; Cui, Q.; Morokuma, K.; Malick, D.K.; Rabuck, A.D.; Raghavachari, K.; Foresman, J.B.; Cioslowski, J.; Ortiz, J.V.; Baboul, A.G.; Stefanov, B.B.; Liu, G.; Liashenko, A; Piskorz, P.; Komaromi, I.; Gomperts, R.; Martin, R.L.; Fox, D.J.; Keith, T.; Al-Laham, M.A.; Peng, C.Y.; Nanaykkara, A.; Challacombe, M.; Gill, P.M.W.; Johnson, B.; Chen, W.; Wong, M.W.; Andres, J.L.; Gonzalez, C.; Head-Gordon, M.; Replogle, E.S.; Pople, J.A. "Gaussian 98, Revision A.9," Gaussian, Inc.

(13) Schlegal, H. Bernhard; "Optimization of Equilibrium Geometries and Transition Structures;" *Journal of Computational Chemistry*, vol 3, p 214-218 (1982).

(14) Jensen, Frank, "Chapter 9. Wave Function Analysis" in *Introduction to Computational Chemistry*; John Wiley & Sons: New York, 1999; pp 217-234.

(15) Mulliken, R.S.; "Electronic Population Analysis on LCAO-MO Molecular Wave Functions. I;" *Journal of Chemical Physics*, vol 23, p 1833-40 (1955).

(16) Hehre, Warren J.; Radom, Leo; Schleyer, Paul v. R.; Pople, John A., "Section 2.8 Mulliken Population Analysis" in *Ab Initio Molecular Orbital Theory*; John Wiley and Sons: New York, 1986; pp 25-29.

(17) Mulliken, R.S.; "Electronic Population Analysis on LCAO-MO Molecular Wave Functions. II. Overlap Populations, Bond Orders, and Covalent Bond Energies.;" *Journal of Chemical Physics*, vol 23, p 1841-46 (1955).

(18) Mulliken, R.S.; "Electronic Population Analysis on LCAO-MO Molecular Wave Functions. III. Effects on Overlap and Gross AO Populations;" *Journal of Chemical Physics*, vol 23, p 2338-42 (1955).

(19) Mulliken, R.S.; "Electronic Population Analysis on LCAO-MO Molecular Wave Functions. IV. Bonding and Antibonding in LCAO and Valence-Bond Theories;" *Journal of Chemical Physics*, vol 23, p 2343-46 (1955).

(20) Momany, Frank A.; "Determination of Partial Atomic Charges from Ab Initio Molecular Electrostatic Potentials. Application to Formamide, Methanol, and Formic Acid;" *Journal of Physical Chemistry*, vol 82, p 592-601 (1978).

(21) Cox, S.R.; Williams, D.E.; "Representation of the Molecular Electronic Potential by a Net Atomic Charge Model;" *Journal of Computational Chemistry*, vol 2, p 304-323 (1981).

(22) Chirlian, Lisa Emily; Francl, Michelle Miller; "Atomic Charges Derived from Electrostatic Potentials: A Detailed Study;" *Journal of Computational Chemistry*, vol 8, p 894-905 (1987).

(23) Breneman, Curt M.; Wiberg, Kenneth B.; "Determining Atom-Centered Monopoles from Molecular Electrostatic Potentials. The Need for High sampling Density in Formamide Conformational Analysis;" *Journal of Computational Chemistry*, vol 11, p 361-373 (1990).

(24) Reed, Alan E.; Weinstock, Robert B.; Weinhold, Frank; "Natural Population Analysis;" *Journal of Chemical Physics*, vol 83, p 735-46 (1985).

(25) Reed, Alan E.; Curtiss, Larry A.; Weinhold, Frank; "Intermolecular Interactions from a Natural Bond Orbital, Donor-Acceptor Viewpoint;" *Chemical Reviews*, vol 88, p 899-926 (1988).

(26) Wiberg, Kenneth B.; "Comparison of Atomic Charges Derived via Different Procedures;" *Journal of Computational Chemistry*, vol 14, p 1504-18 (1993).

(27) Corbridge, D.E.C., "Phosphorus: An Outline of Its Chemistry, Biochemistry, and Uses" ; 5th ed.; Elsevier: Amsterdam, 1995; p 138.

(28) Corbridge, D.E.C., "Phosphorus: An Outline of Its Chemistry, Biochemistry, and Uses" ; 5th ed.; Elsevier: Amsterdam, 1995; p 155.

(29) Ochterski, Joseph W. "Thermochemistry in Gaussian," Gaussian, Inc.; internal white paper, April, 2000.

(30) Hinchliffe, Alan, in *Computational Quantum Chemistry*; John Wiley and Sons: New York, 1988; pp 12 and 38.

(31) Griffiths, James E.; Burg, Anton B.; "The Phosphinous Acid $(CF_3)_2POH$ and Diphosphoxane $(CF_3)_2POP(CF_3)_2$;" *Journal of the American Chemical Society*, vol 82, p 1507-8 (1960).

(32) Griffiths, James E.; Burg, Anton B.; "Oxygen Chemistry of the $(CF_3)_2P$ Group: the Diphosphoxane; the Phosphinous Acid, Esters and Related Phosphine Oxides; Phosphinyl Halides and Infrared Spectra;" *Journal of the American Chemical Society*, vol 84, p 3442-50 (1962).

(33) Gay, Ian D.; McFarlan, A.J.; Morrow, B.A.; "Trimethyl Phosphite Adsorbed on Silica: An NMR and Infrared Study;" *Journal of Physical Chemistry*, vol 95, p 1360-8 (1991).

(34) Raevskii, O.A.; Donskaya, Yu. A.; Chirkova, L.P.; "Hindered Internal Rotation and Raman Spectra of Trimethyl Phosphite;" *Bulletin of the Academy of Sciences of the U.S.S.R. -- Division of Chemical Sciences*, p 571-5 (1980).

(35) Pople, John A.; Head-Gordon, Martin; Fox, Douglas J.; Raghavachari, Krishnan; Curtis, Larry A.; "Gaussian-1 Theory: A General Procedure for Prediction of Molecular Energies;" *Journal of Chemical Physics*, vol 90, p 5622-29 (1989).

(36) Curtis, Larry A.; Raghavachari, Krishnan; Trucks, Garry W.; Pople, John A.; "Gaussian-2 Theory for Molecular Energies of First and Second-row Compounds;" *Journal of Chemical Physics*, vol 94, p 7211-30 (1991).

(37) Ochterski, Joseph W.; Petersson, G.A.; J.A. Montgomery, Jr.; "A Complete Basis Set Model Chemistry V. Extensions to Six or More Heavy Atoms;" *Journal of Chemical Physics*, vol 104, p 2598-2619 (1996).

(38) Ochterski, Joseph W.; Petersson, George A.; Wiberg, Kenneth B.; "A Comparison of Model Chemistries;" *Journal of the American Chemical Society*, vol 117, p 11299-11308 (1995).

(39) Foresman, James B.; Frisch, Æleen, "Chapter 7. High Accuracy Energy Models" in *Exploring Chemistry with Electronic Structure Methods, 2nd edition*; Gaussian, Inc.: Pittsburgh, PA, 1996; pp 141-161.

(40) Meyrick, C.I.; Thompson, H.W.; "Vibrational Spectra of Alkyl Esters of Phosphorus Oxy-acids;" *Journal of the Chemical Society*, p 225-9 (1950).

(41) Fritzowsky, Norbert; Lentz, A.; Goubeau, J.; "Schwingungsspektren und Kraftkonstanten der Ubergangsreihe $P(OCH_3)_3$--PCl_3;" *Zeitscrit Anorg Allg Chem*, vol 386, p 203-7 (1971).

(42) Fritzowsky, Norbert; Lentz, A.; Goubeau, J.; "Schwingungsspektren und Kraftkonstanten der Ubergangsreihe PCl_3 --$P(SCH_3)_3$;" *Zeitscrit Anorg Allg Chem*, vol 386, p 67-72 (1971).

(43) Pouchert, Charles J., "Trimethyl Phosphite (Vapor)" in *The Aldrich Library of FT-IR Spectra*; 1st ed.; Aldrich Chemical Do.: Milwaukee, WI, 1995; Vol. 3; p 838B.

(44) Pouchert, Charles J., "Trimethyl Phosphite (Liquid)" in *The Aldrich Library of FT-IR Spectra*; 1st ed.; Aldrich Chemical Do.: Milwaukee, WI, 1995; Vol. 1; p 910A.

(45) Foresman, James B.; Frisch, Æleen, "Frequencies and Intensities" in *Exploring Chemistry with Electronic Structure Methods, 2nd edition*; Gaussian, Inc.: Pittsburgh, PA, 1996; pp 63-4.

(46) Socrates, George, *Infrared and Raman Characteristic Group Frequencies*; 3rd ed.; John Wiley & Sons: New York, 2001.

(47) Socrates, George, "Chapter 7. Organic Phosphorus Compounds" in *Infrared and Raman Characteristic Group Frequencies*; 3rd ed.; John Wiley & Sons: New York, 2001; p 229.

(48) Guilbault, George E.; Scheide, E.; Das, J.; "An Experimental Technique for Studying the Infrared Spectrum of Chemisorbed Compounds;" *Spectroscopy Letters*, vol 1, p 167-175 (1968).

(49) Verken, B.J. Van der; Herman, M.A.; "Vibrational Spectra of $CH_3PO(OCH_3)_2$ and Isotopically Substituted Derivatives;" *Phosphorus and Sulfur*, vol 10, p 357-368 (1981).

(50) Verken, B. J. Van der; Herman, M.A.; "Conformational Analysis of Dimethyl Methylphosphonate;" *Journal of Molecular Structure*, vol 42, p 161-170 (1977).

(51) Hameka, Hendrik F.; Jensen, James O.; Carrieri, Arthur H. "Theoretical Predictions of the Infrared and Raman Spectra of Some Phosphorus Containing Simulants," Chemical Research Development and Engineering Center; CRDEC-TR-327, March 1992, Unclassified Report (ADA253962).

(52) Hameka, Hendrik F.; Carrieri, Arthur H.; Jensen, James O.; "Calculations of the Structure and the Vibrational Infrared Frequencies of Some Methylphosphonates;" *Phosphorus, Sulfur, and Silicon*, vol 66, p 1-11 (1992).

(53) Hoffland, Lynn D.; Piffath, Ronald J.; Bouck, James B.; "Spectral Signatures of Chemical Agents and Simulants;" *Optical Engineering*, vol 24, p 982-4 (1985).

(54) Weast, Robert C.; Grasselli, Jeanett G., "HODOC No:19803" in *Handbook of Data on Organic Compounds*; 2nd Edition ed.; CRC Press, Inc.: Boca Raton, 1989; Vol. 5.

(55) Pouchert, Charles J., "913D Bis(2-Ethylhexyl) phosphonate" in *The Aldrich Library of FT-IR Spectra*; Aldrich Chemical Do.: Milwaukee, WI, 1995; Vol. 1.

(56) Melius, Carl F.; Allendorf, Mark D.; "Bond Additivity Corrections for Quantum Methods;" *Journal of Physical Chemistry A*, vol 104, p 2168-77 (2000).

(57) Allendorf, Mark D.; Melius, Carl F.; Cosic, Biljana; Fontijn, Arthur; "BAC-G2 Predictions of Thermochemistry for Gas-Phase Aluminum Compounds;" *Journal of Physical Chemistry A*, vol 106, p 2629-40 (2002).

DEPARTMENT OF THE ARMY
CDR USASBCCOM
ATTN AMSSB SCI C
5183 BLACKHAWK ROAD
APG MD 21010-5424

OFFICIAL BUSINESS

FIRST CLASS